Electrical manipulation of non-collinear antiferromagnet

Shunsuke Fukami[1-5]

[collaborators]
Y. Takeuchi, Y. Yamane, J.-Y. Yoon, R. Itoh, B. Jinnai,
S. Kanai, S. DuttaGupta, J. Ieda, H. Ohno

1. Laboratory for Nanoelectronics and Spintronics, RIEC, Tohoku Univ.
2. WPI-Advanced Institute for Materials Research, Tohoku Univ.
3. Center for Spintronics Research Network, Tohoku Univ.
4. Center for Science and Innovation in Spintronics, Tohoku Univ.
5. Center for Innovative Integrated Electronic Systems, Tohoku Univ.

TOHOKU UNIVERSITY

JAEA

RIEC

AIMR

CSIS

FRIS

CSRN

cies

A portion of this work has been supported by the R&D Project for ICT Key Technology of MEXT, ImPACT Program of CSTI, JST-CREST JPMJCR19K3, JSPS Kakenhi 17H06093 and 19H05622.

Outline

1. Introduction
   - Electrical manipulation of magnetic materials
   - Non-collinear antiferromagnet
2. Chiral-spin rotation of non-collinear antiferromagnet Mn_3Sn
   - Preparation of epitaxial thin film
   - Chiral-spin rotation
   - Analysis of domain size
   - Mn_3Sn thickness dependence
3. Summary

Electrical manipulation of magnetic materials

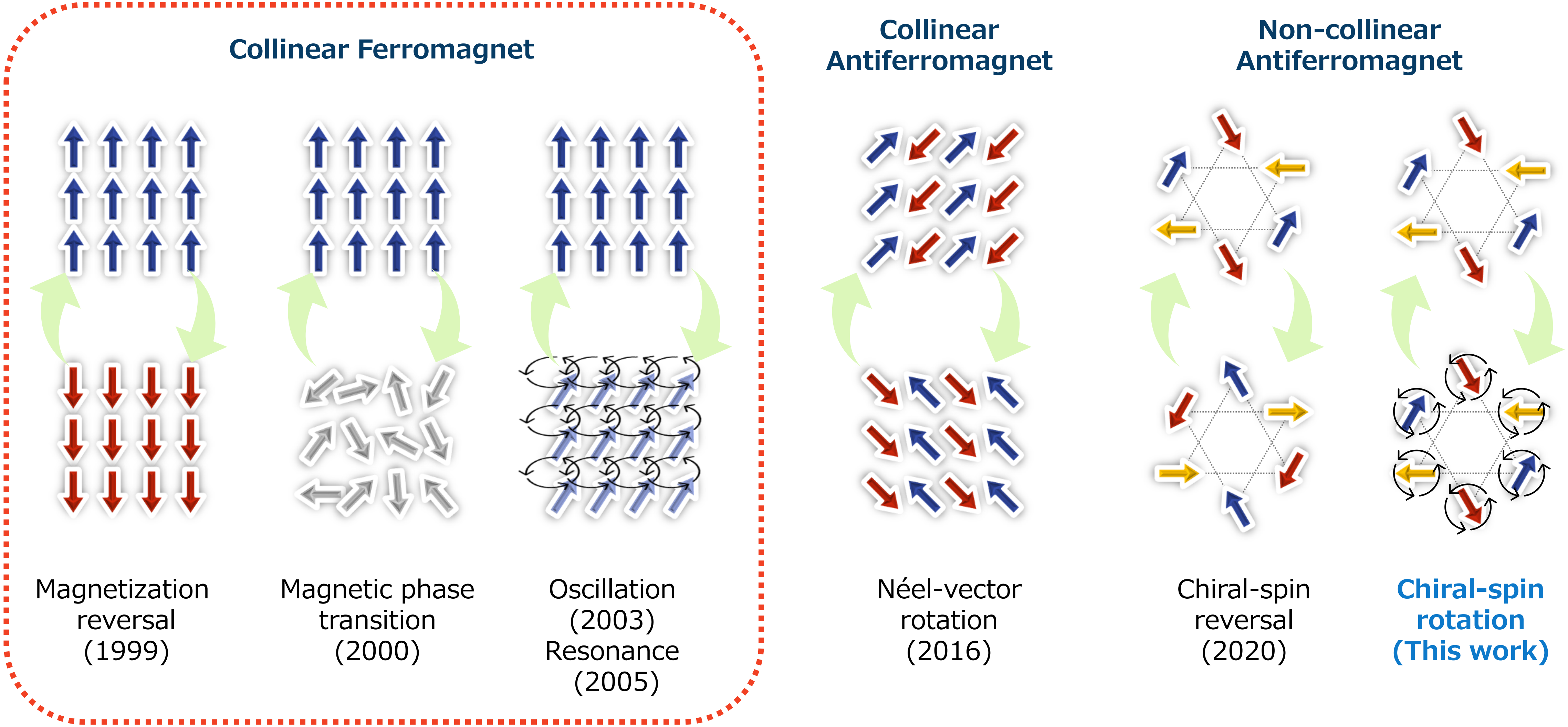

Magnetization reversal

- **STT-induced magnetization switching**

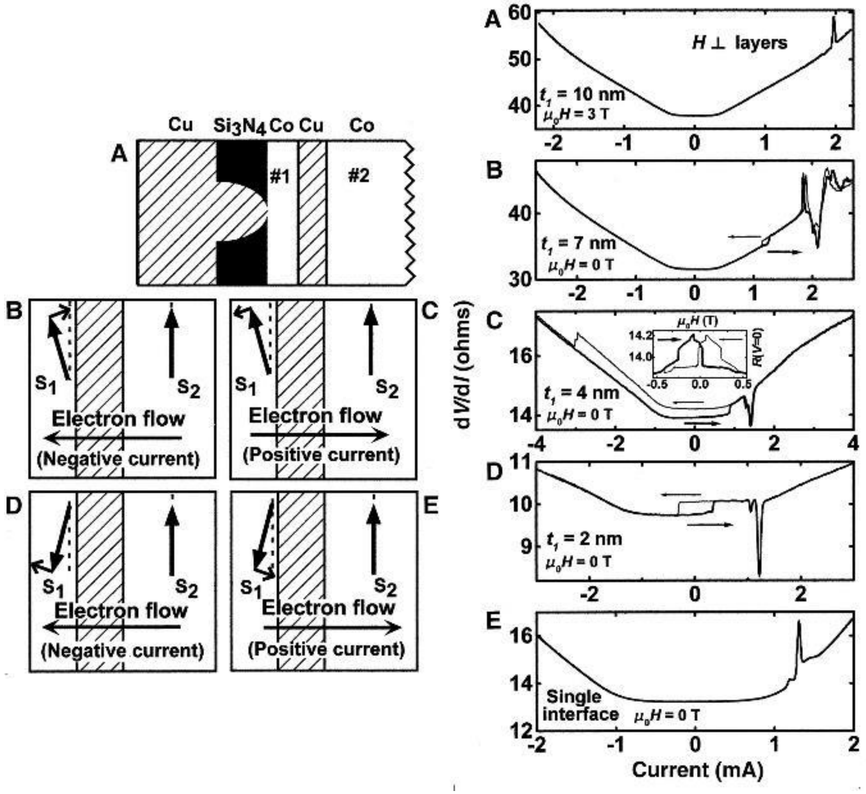

E. B. Myers *et al.*, Science **285**, 867 (1999).

- **Perpendicular CoFeB/MgO MTJ**

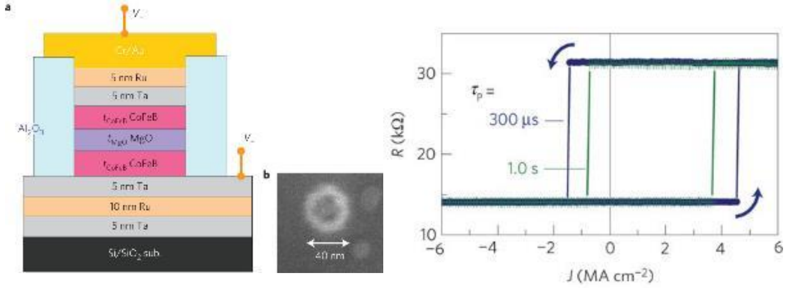

S. Ikeda *et al.*, NMAT **10**, 721 (2010).

- **Current-induced DW motion**

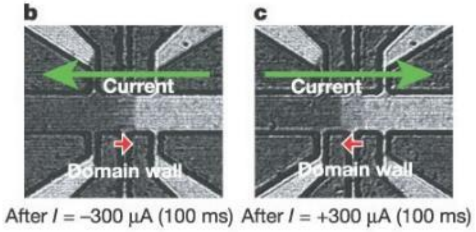

M. Yamanouchi *et al.*, Nature **428**, 539 (2004).

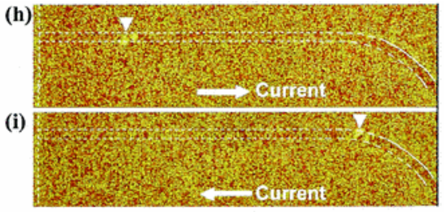

M. Yamaguchi *et al.*, PRL **92**, 077205 (2004).

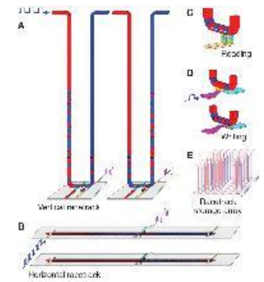

S. S. P. Parkin *et al.*, Science **320**, 190 (2008).

- **SOT-induced magnetization switching** (Q. Shao *et al.* TMAG **57**, 800439 (2021))

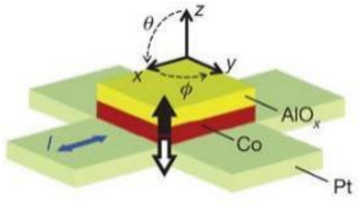

I. M. Miron *et al.*, Nature **476**, 189 (2011).

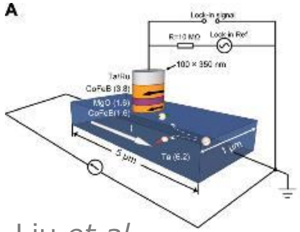

L. Liu *et al.*, Science **336**, 555 (2012).

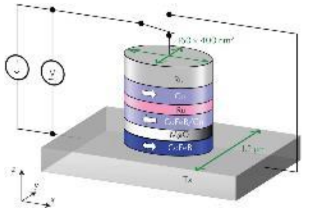

S. Fukami *et al.*, NNANO **11**, 621 (2016).

◆ **STT-MRAM**

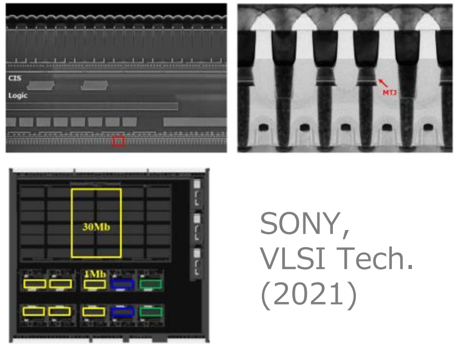

SONY, VLSI Tech. (2021)

Magnetic-phase transition

- **Electric-field control of FM**

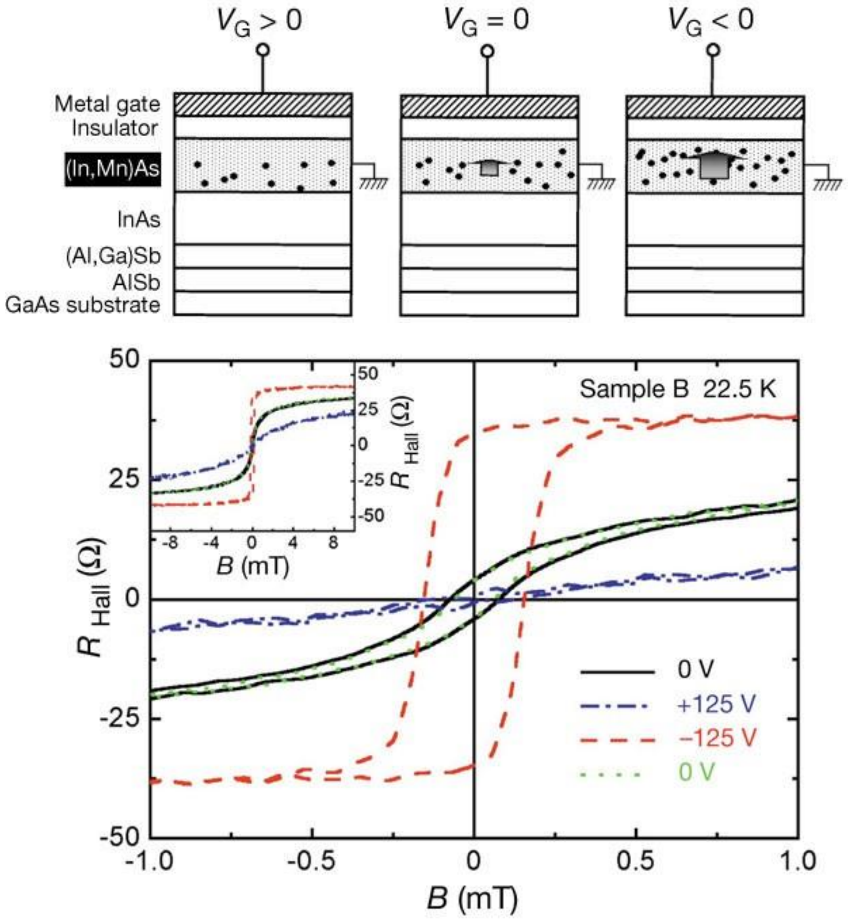

H. Ohno *et al.*, Nature **408**, 944 (2000).

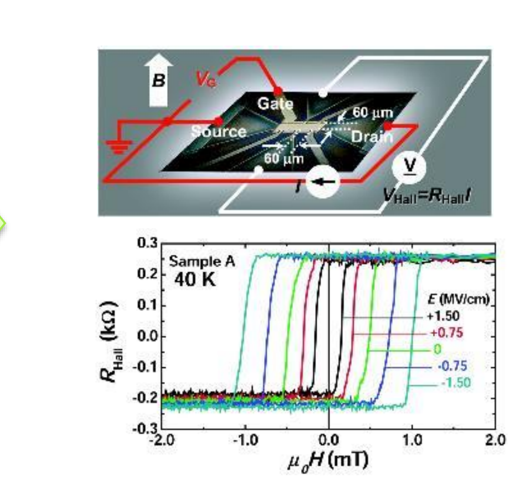

D. Chiba *et al.*, Science **301**, 943 (2003).
D. Chiba *et al.*, Nature **455**, 515 (2008).

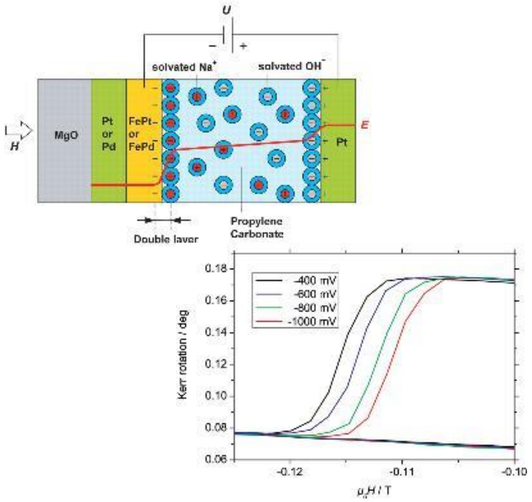

M. Weisheit *et al.*, Science **315**, 349 (2008).

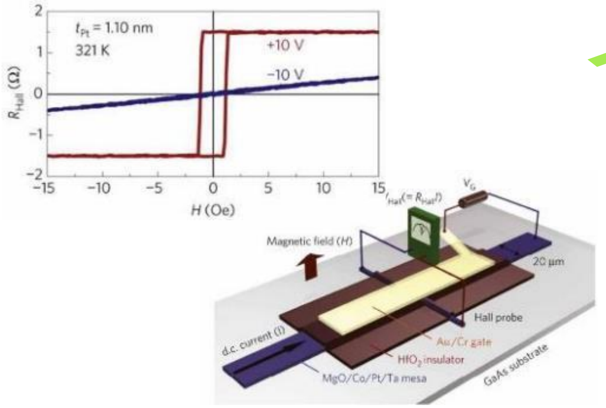

D. Chiba *et al.*, NMAT **10**, 853 (2011).

- **Dynamical switching**

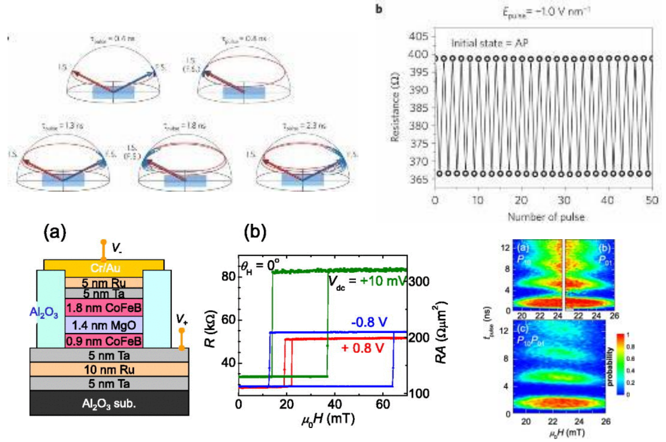

Y. Shiota *et al.*, NMAT **11**, 39 (2012).
S. Kanai *et al.*, APL **101**, 122403 (2012).

Oscillation / Resonance

- **Spin-torque oscillation (dc → rf)**

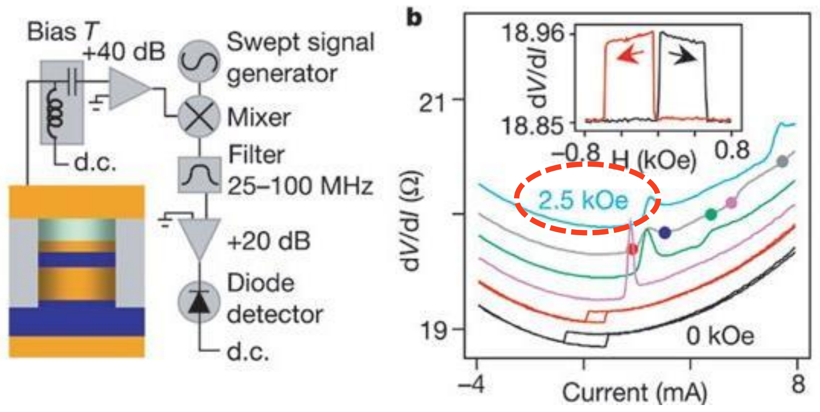

S. I. Kiselev *et al.*, Nature **425**, 380 (2003).

- **Spin-torque FMR (rf → dc)**

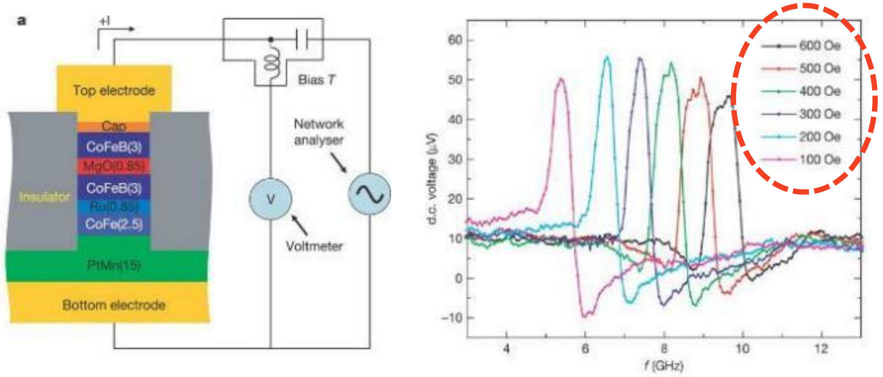

A. A. Tulapurkar *et al.*, Nature **438**, 339 (2005).

- **Phase locking (synchronization)**

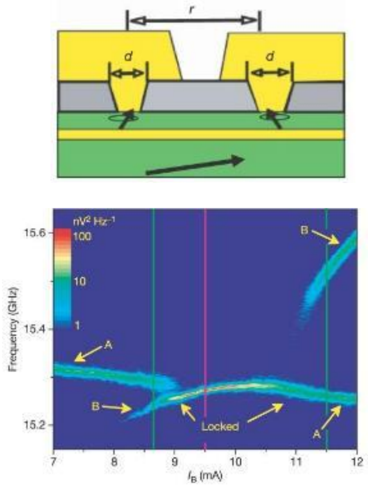

S. Kaka *et al.*,
Nature **437**, 389 (2005).

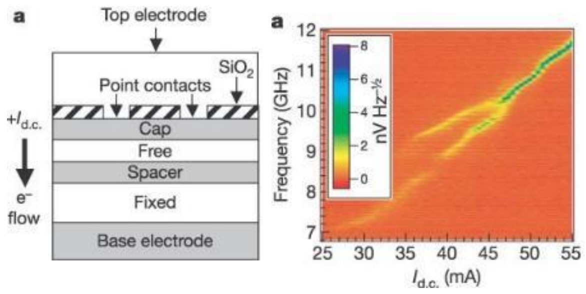

F. B. Mancoff *et al.*,
Nature **437**, 393 (2005).

- **Neuromorphic computing**

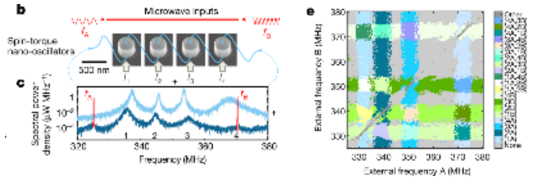

M. Romera *et al.*, Nature **563**, 230 (2018).

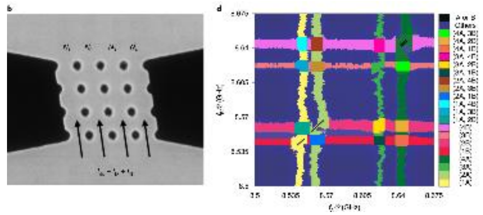

M. Zahedinejad *et al.*, NNANO **15**, 47 (2020).

- **Communication, harvesting**

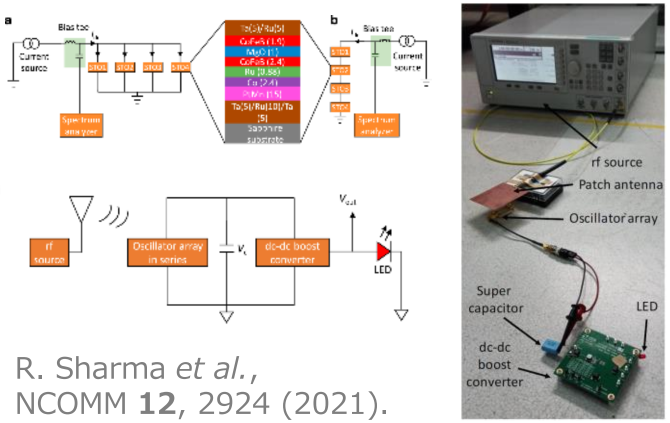

R. Sharma *et al.*,
NCOMM **12**, 2924 (2021).

Electrical manipulation of magnetic materials

Collinear Ferromagnet

Collinear Antiferromagnet

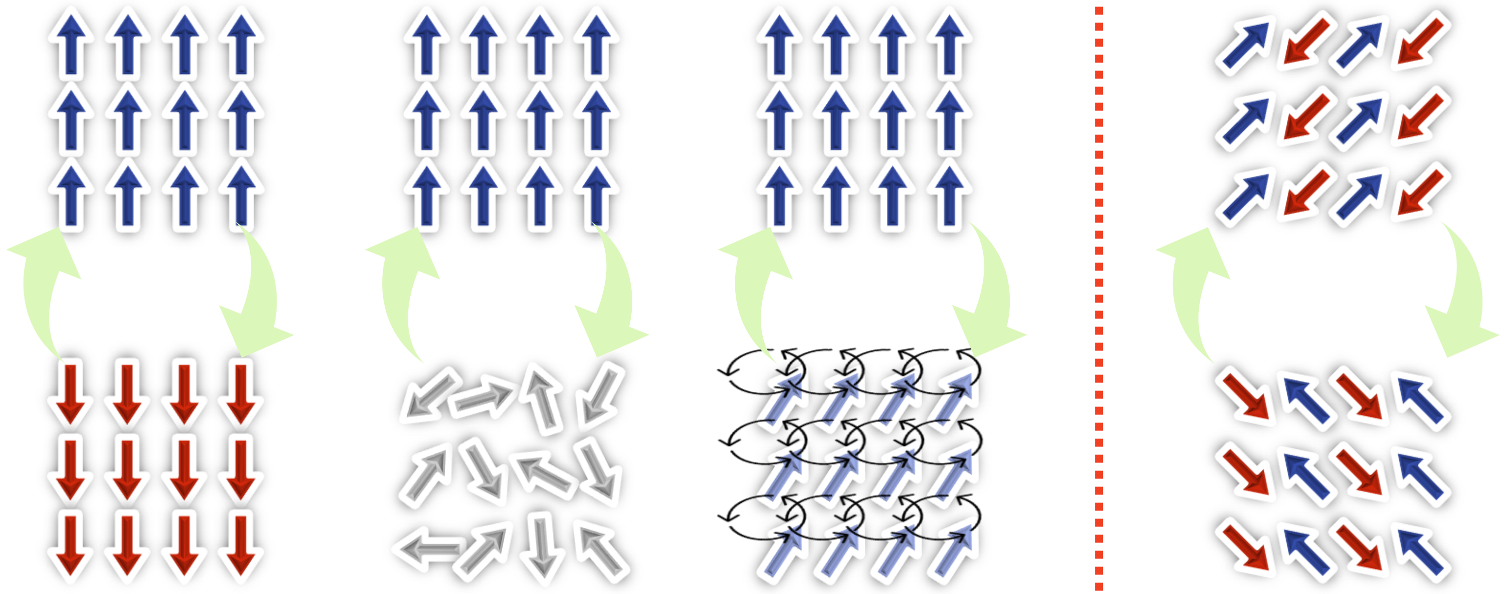

Magnetization reversal (1999)

Magnetic phase transition (2000)

Oscillation (2003) Resonance (2005)

Néel-vector rotation (2016)

Néel-vector rotation

- **Néel-vector rotation in CuMnAs**

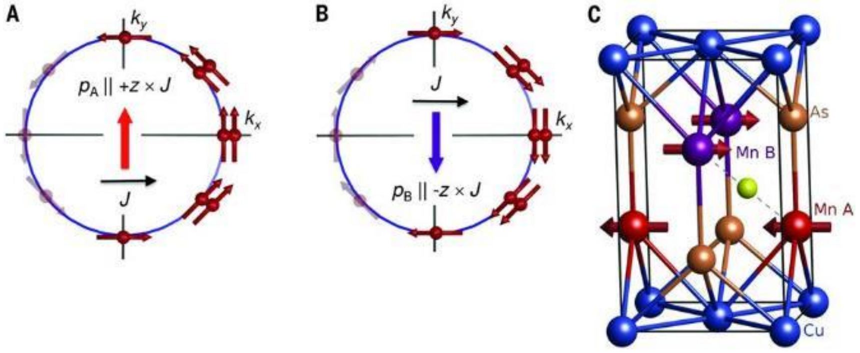

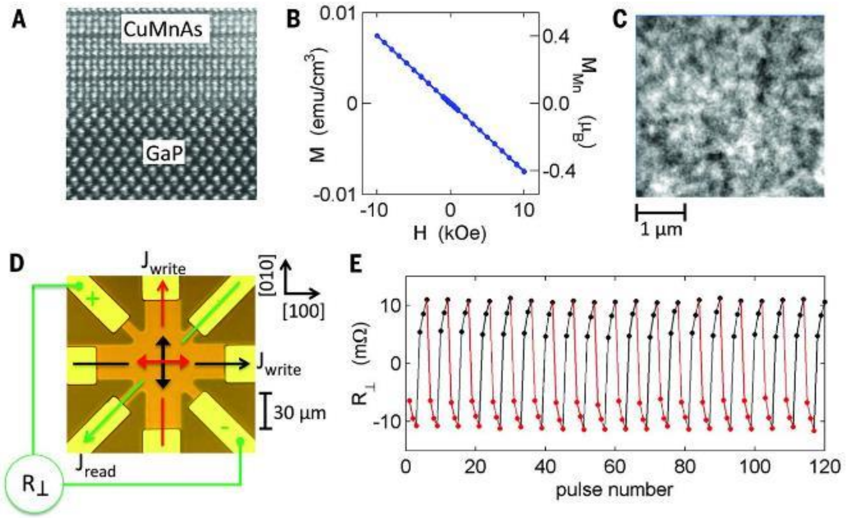

P. Wadley *et al.*, Science **351**, 587 (2016).

- **Mn_2Au**

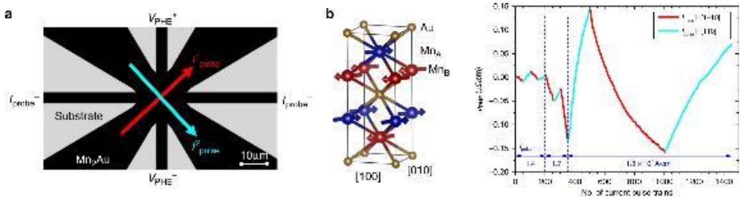

S.Yu Bodnar *et al.*, NCOMM **9**, 348 (2018).

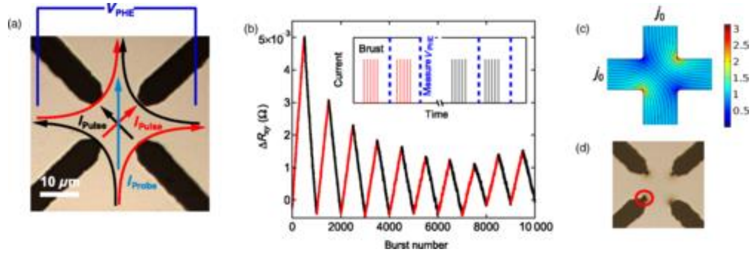

M. Meinert *et al.*, PRAp **9**, 064040 (2018).

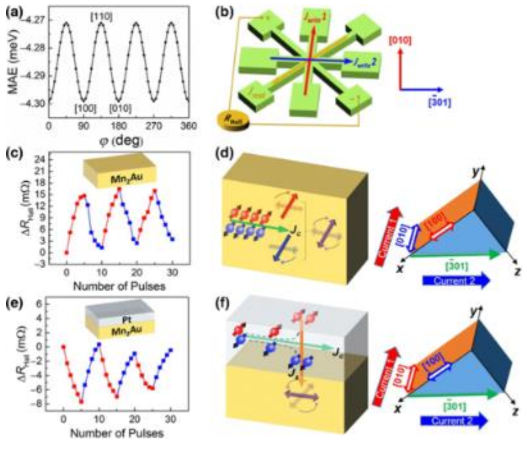

X.F. Zhou *et al.*, PRAp **11**, 054030 (2019).

- **NiO**

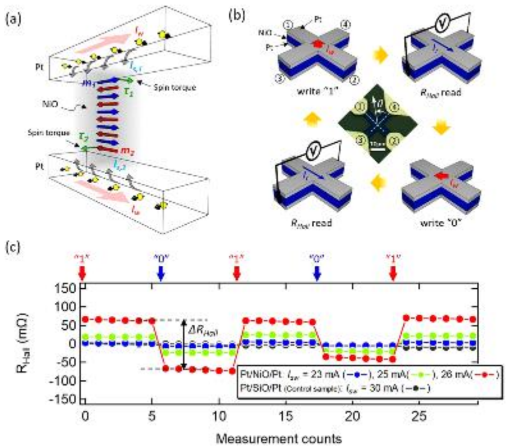

T. Moriyama *et al.*, SREP **8**, 14167 (2018).

- **PtMn**

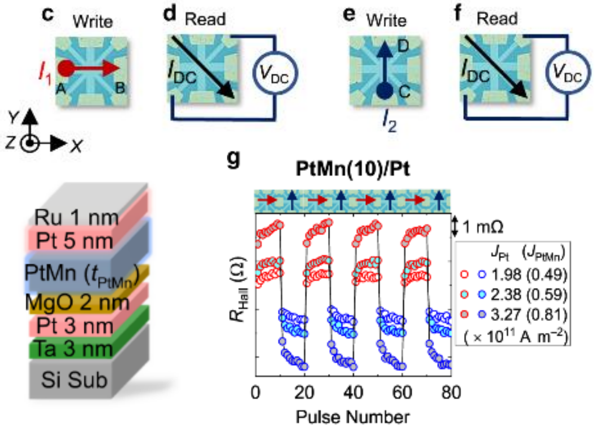

S. DuttaGupta *et al.*, NCOMM **11**, 5715 (2020).

Electrical manipulation of magnetic materials

Collinear Ferromagnet | **Collinear Antiferromagnet** | **Non-collinear Antiferromagnet**

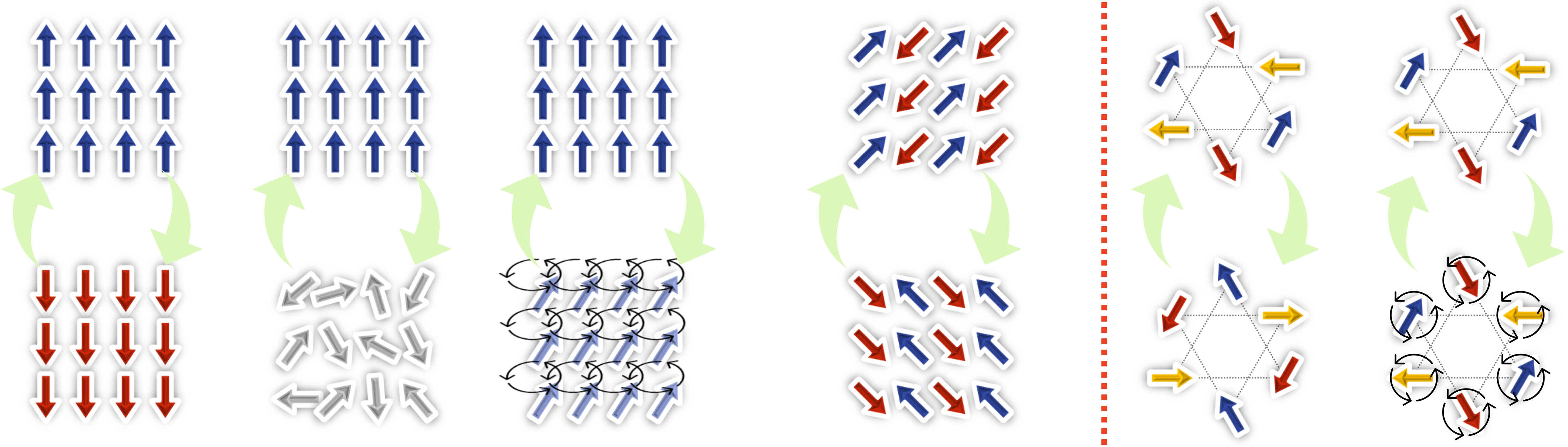

Magnetization reversal (1999)

Magnetic phase transition (2000)

Oscillation (2003) Resonance (2005)

Néel-vector rotation (2016)

Chiral-spin reversal (2020)

Chiral-spin rotation (This work)

Non-collinear antiferromagnets

Behaves like ferromagnet despite negligible magnetization

Theory

Experiment

*L*1$_2$-Mn$_3$Ir

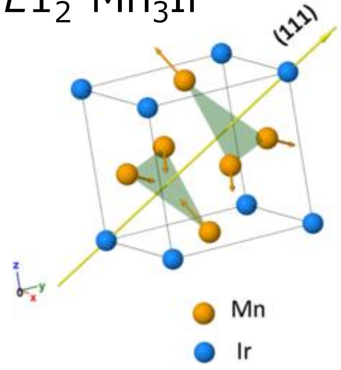

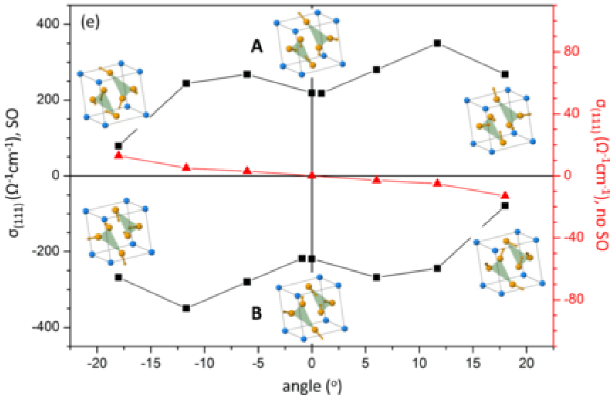

H. Chen *et al.*, PRL **112**, 017205 (2014).

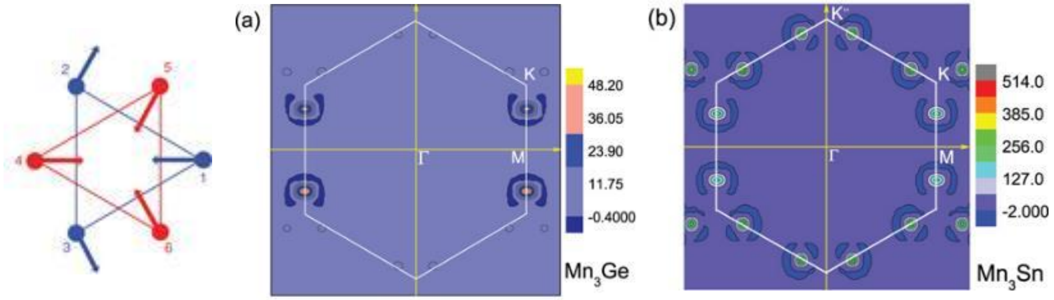

J. Kübler & C. Felser, EPL **108** 67001 (2014).

*D*0$_{19}$-Mn$_3$Sn

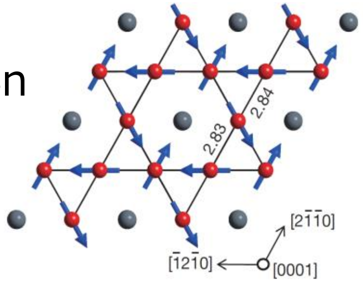

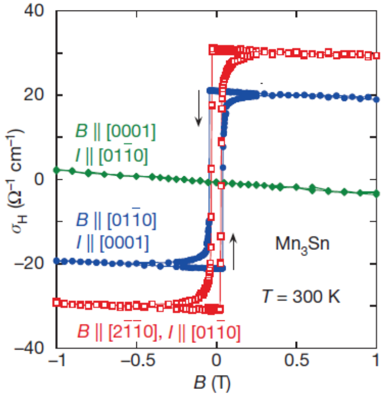

S. Nakatsuji *et al.*,
Nature **527**, 212 (2015).

*D*0$_{19}$-Mn$_3$Ge

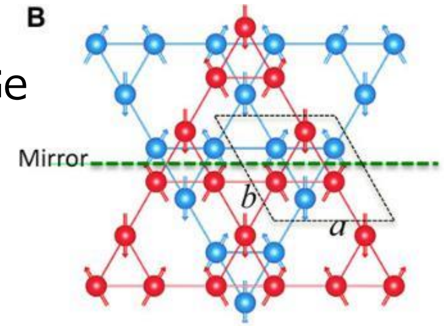

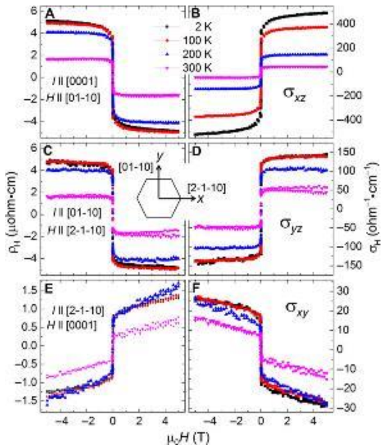

A. K. Nayak et al.,
Sci.Adv. **2**, e1501870 (2016).

Large anomalous Hall effect due to non-vanishing Berry curvature

ANE, MOKE

Anomalous Nernst Effect (ANE)

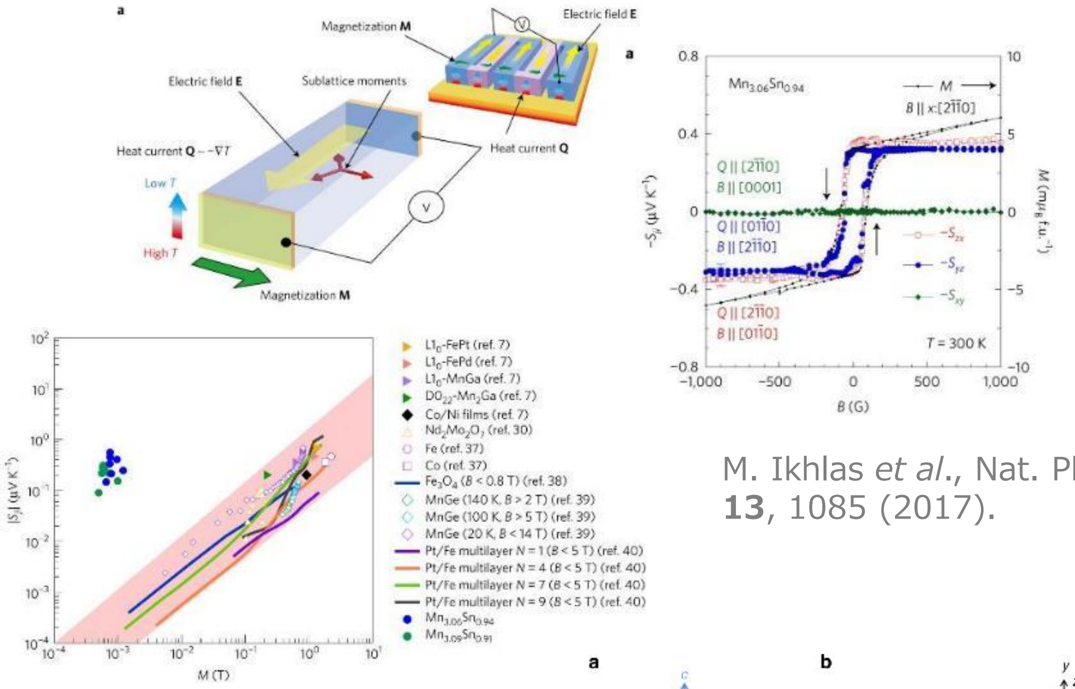

M. Ikhlas *et al*., Nat. Phys. **13**, 1085 (2017).

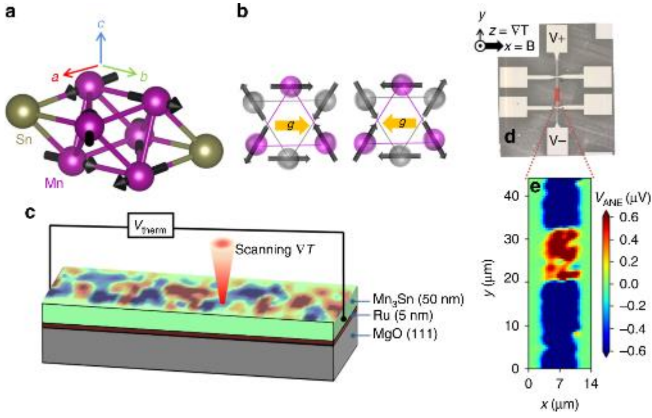

H. Reichlova *et al*., NCOMM **10**, 5459 (2019).

Magneto-Optical Kerr Effect (MOKE)

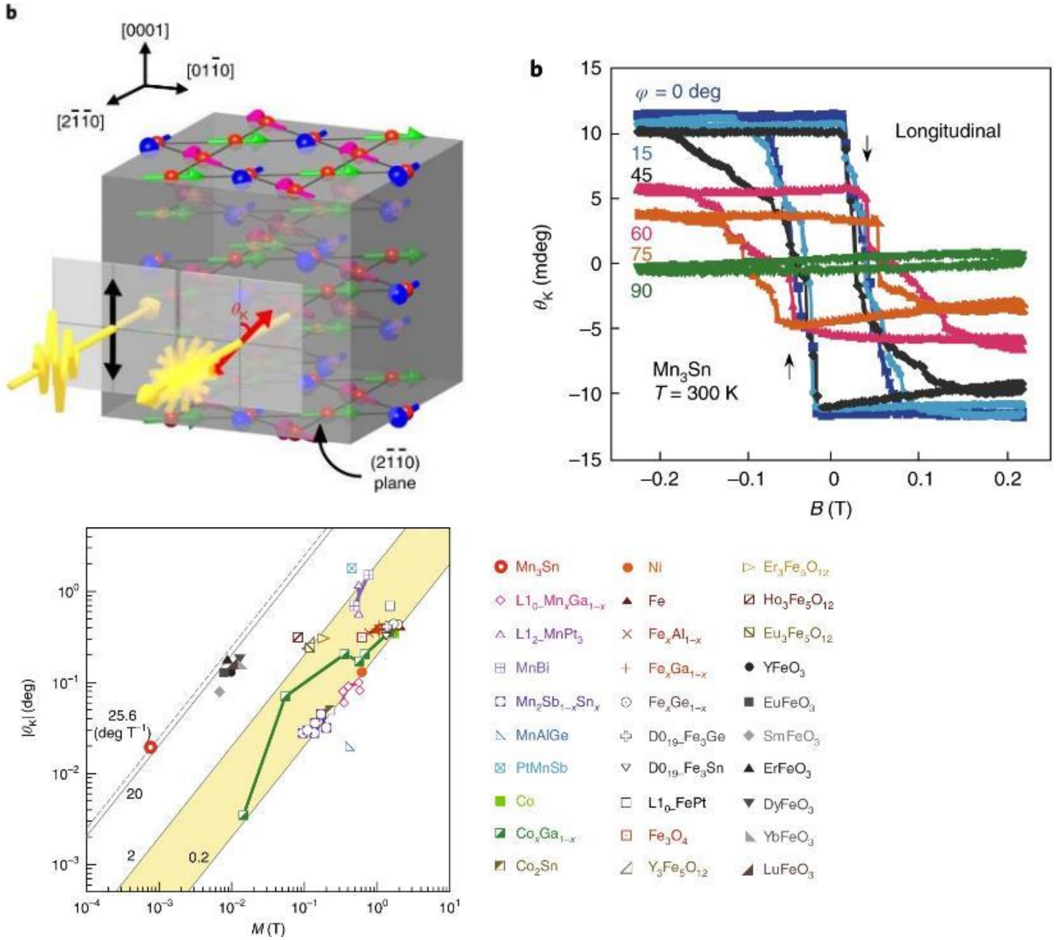

T. Higo *et al*., Nat. Photo. **12**, 73 (2018).

Chiral-spin reversal

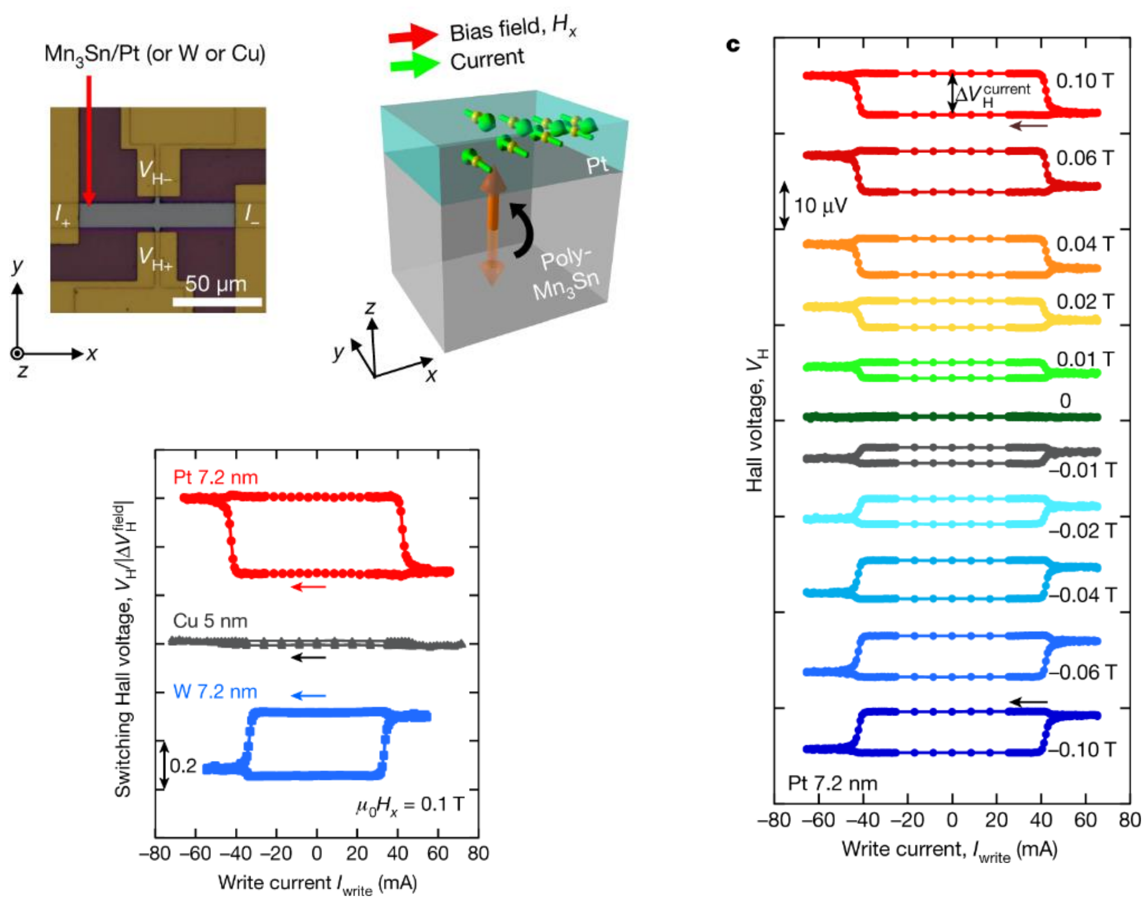

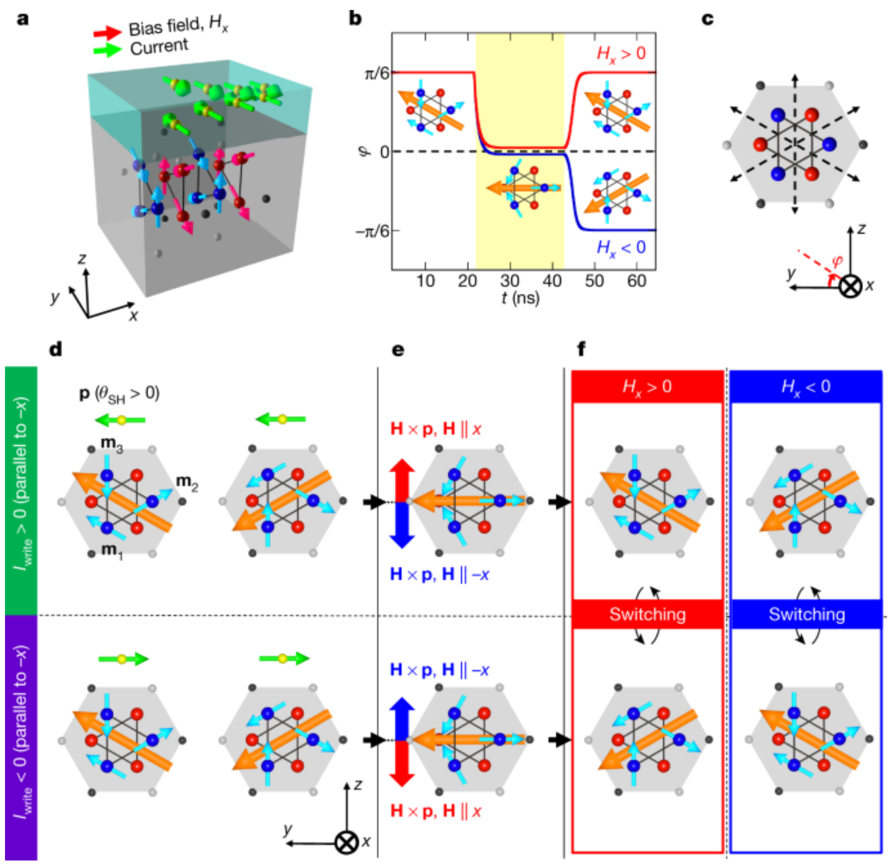

H. Tsai *et al.*, Nature **580**, 608 (2020).

Same protocol as SOT-induced magnetization switching

Any characteristic phenomena in NC-AFM?

Chiral-spin rotation – characteristic phenomenon in NC-AFM

LOW TEMPERATURE PHYSICS VOLUME 41, NUMBER 9 SEPTEMBER 2015

Using generalized Landau-Lifshitz equations to describe the dynamics of multi-sublattice antiferromagnets induced by spin-polarized current

O. V. Gomonay[a)]

National Technical University of Ukraine "KPI," 37 Peremogy Ave., Kiev 03056, Ukraine

V. M. Loktev

National Technical University of Ukraine "KPI," 37 Peremogy Ave., Kiev 03056, Ukraine and Bogolyubov Institute for Theoretical Physics, NASU, 14b Metrologicheskaya St., Kiev 03680, Ukraine

(Submitted May 8, 2015)
Fiz. Nizk. Temp. **41**, 898–907 (September 2015)

Antiferromagnets (AFM) with a zero, or very small macroscopic magnetization, are promising materials in spintronics. Based on generalized Landau-Lifshitz equations, we examine the magnetic dynamics of three-sublattice AFM in the presence of a spin-polarized current, and in particular, the switching processes between different equilibrium states. We found the conditions for effective switching by pulsed and DC, as well as by an external magnetic field. We examined the features of stationary dynamic states, caused by the current. The obtained results can be used to develop high-speed elements of AFM-based memory materials. © *2015 AIP Publishing LLC*.
[http://dx.doi.org/10.1063/1.4931648]

$L1_2$-Mn_3Ir

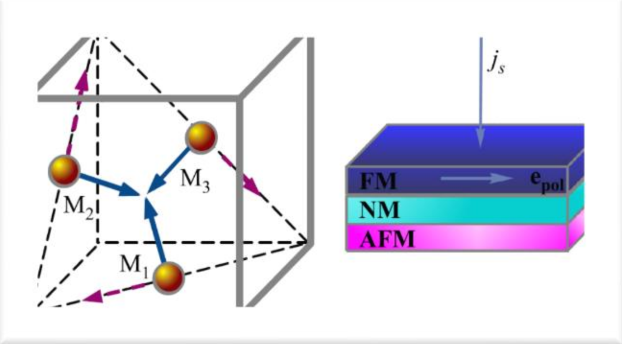

or to simultaneously turn on the current and the magnetic field. Indeed, as seen on the phase diagram of the system with current-field variables (Fig. 5), it is possible to isolate three specific ranges of parameters, in which (i): there are two points of stable equilibrium; (ii) only one point of rest is stable; (iii) there are no points of rest, but as we will see below, there exist stationary states in which the AFM vectors rotate in the plane (111). The lines separating these regions are defined by

$$\frac{j_s}{j_0^{cr2}} = \left(\frac{3H}{2H_{cr}} \pm \sqrt{2 + \left(\frac{H}{2H_{cr}}\right)^2}\right) \times \sqrt{\frac{1}{2} - 2\left(\frac{H}{4H_{cr}}\right)^2 \pm 2\frac{H}{4H_{cr}}\sqrt{\frac{1}{2} + \left(\frac{H}{4H_{cr}}\right)^2}}, \quad (30)$$

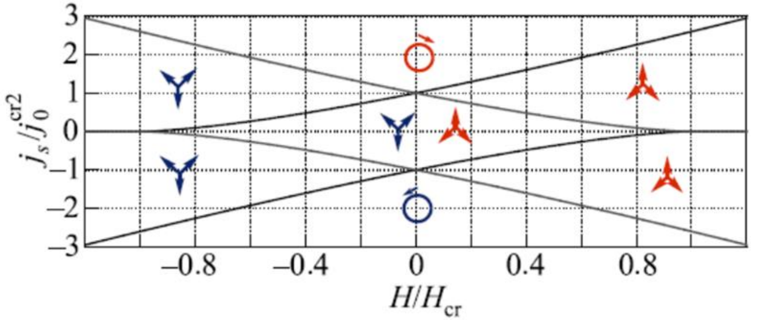

FIG. 5. The state diagram with field-current density variables. Equilibrium states 1 and 2 are differentiated by a rotation of 180° in the (111) plane, depicted by arrows. Circles denote the area of steady state precession in its direction.

O. V. Gomonay and V. M. Loktev, Low Temp Phys. **41**, 698 (2015).

Electrical manipulation of magnetic materials

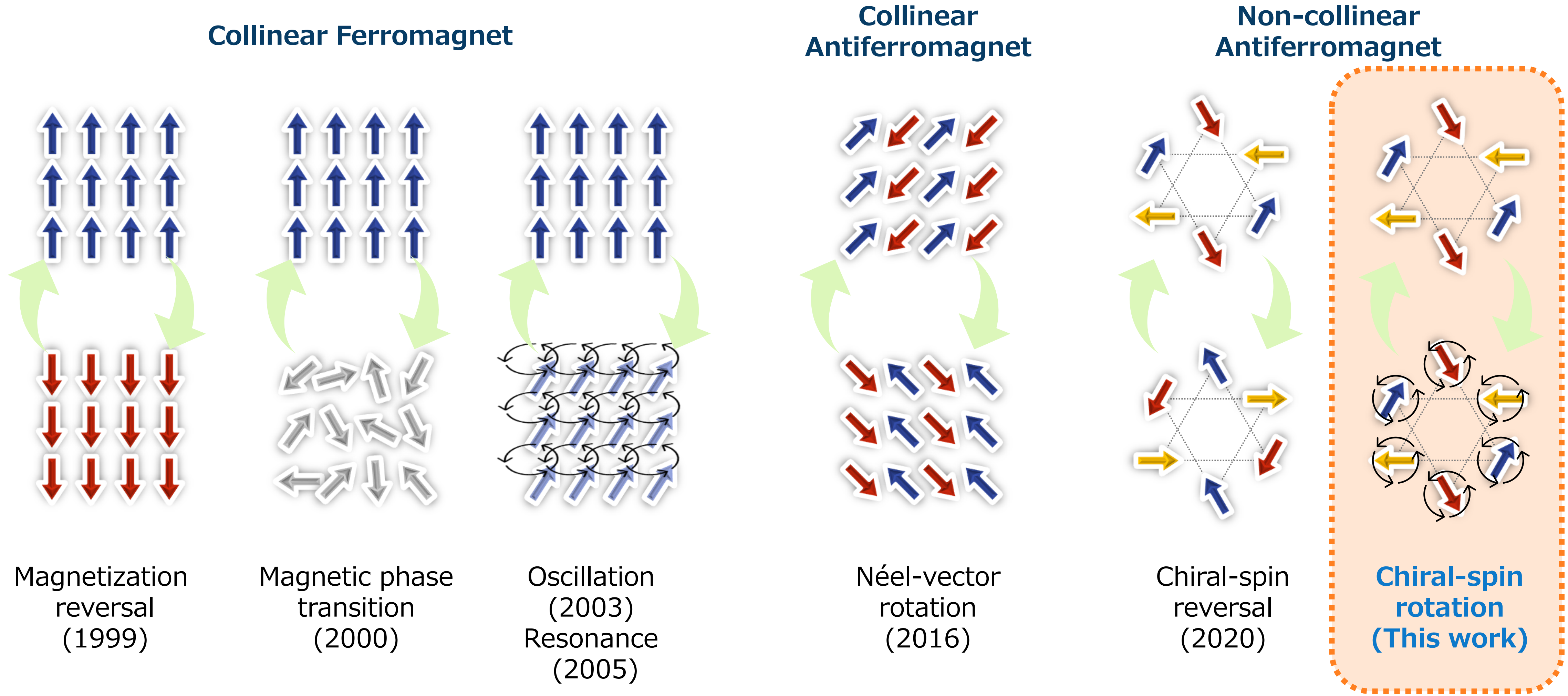

Outline

1. Introduction
   - Electrical manipulation of magnetic materials
   - Non-collinear antiferromagnet
2. Chiral-spin rotation of non-collinear antiferromagnet Mn_3Sn
   - Preparation of epitaxial thin film
   - Chiral-spin rotation
   - Analysis of domain size
   - Mn_3Sn thickness dependence
3. Summary

Objectives

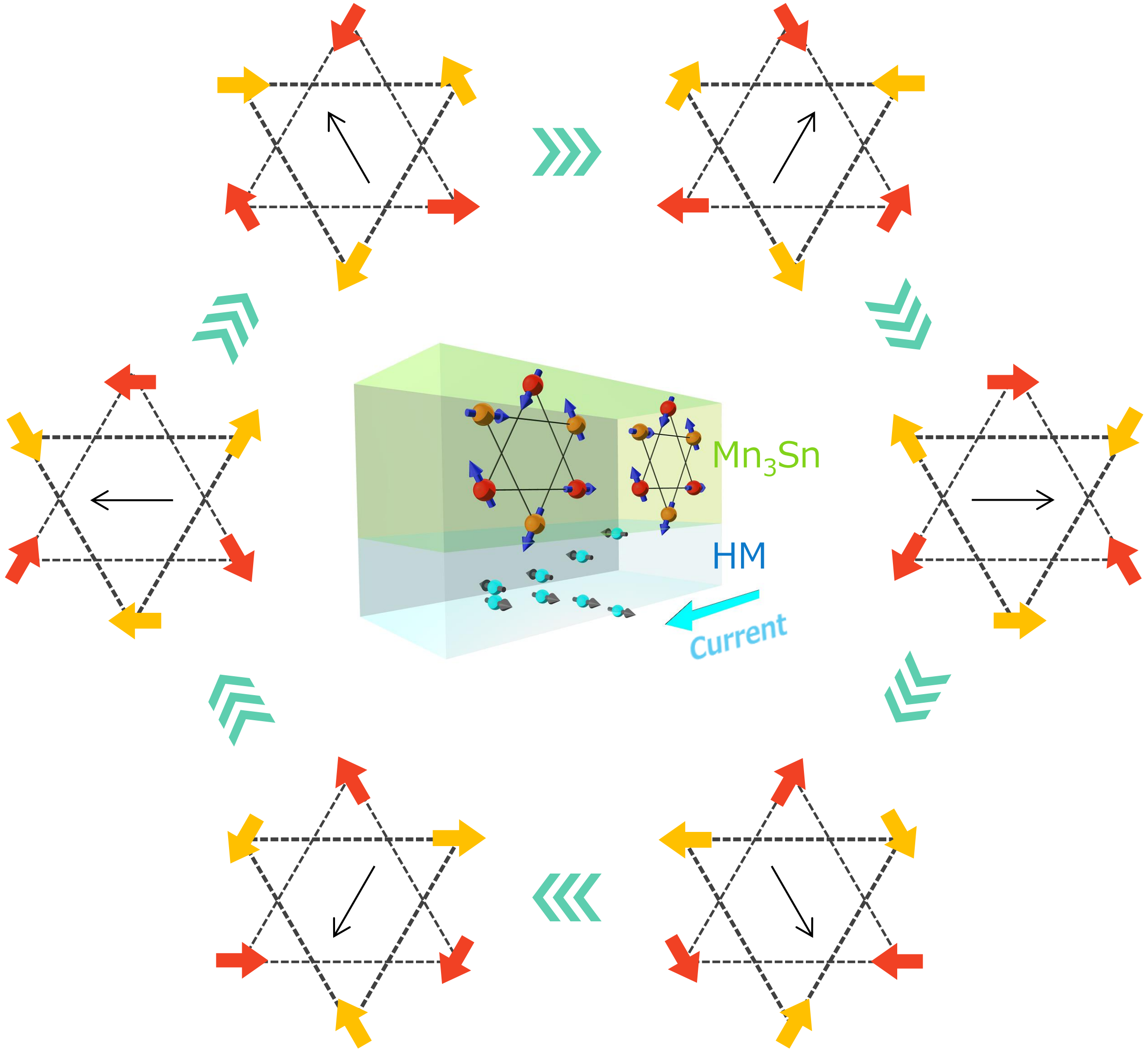

- (Indirect) observation of chiral-spin rotation
- Comparison with chiral-spin reversal
- Effect of multidomain structure
- Thickness dependence

Outline

1. Introduction
   - Electrical manipulation of magnetic materials
   - Non-collinear antiferromagnet
2. Chiral-spin rotation of non-collinear antiferromagnet Mn_3Sn
   - Preparation of epitaxial thin film
   - Chiral-spin rotation
   - Analysis of domain size
   - Mn_3Sn thickness dependence
3. Summary

Stack deposition and characterization

- Layer structure

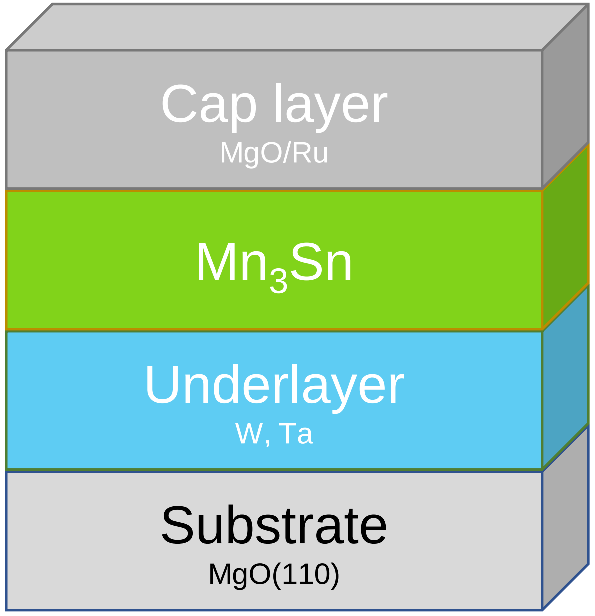

Deposition temperature : 400 ^{o}C
Post annealing temperature : 500 ^{o}C

- Crystal structure analysis
  - XRD
    - "2θ-θ" : Indicating out-of-plane lattice structure
    - "ϕ scan" : Indicating in-plane lattice structure

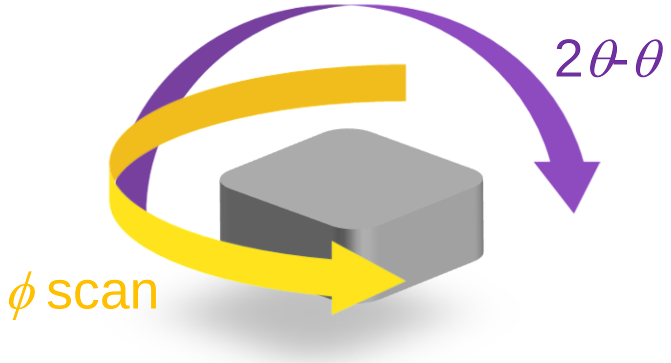

m : Magnetization
$H_{\perp(//)}$: Out of plane (In-plane) magnetic field
R_H : Hall resistance
ρ_H : Hall resistivity

- m - $H_{\perp(//)}$
  - VSM (out, in-plane)
- R_H (ρ_H) - $H_\perp$
  - PPMS

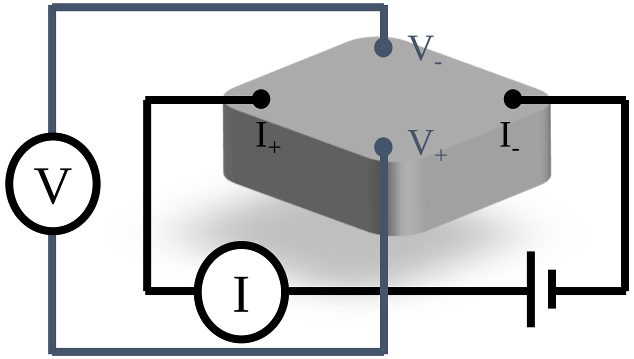

J. Yoon *et al.*, Appl. Phys. Express **13**, 013001 (2020).

Structural characterization by XRD

- Stack structure

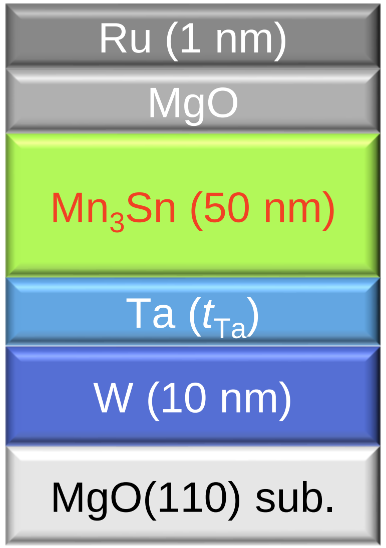

- XRD (2θ-θ scan)

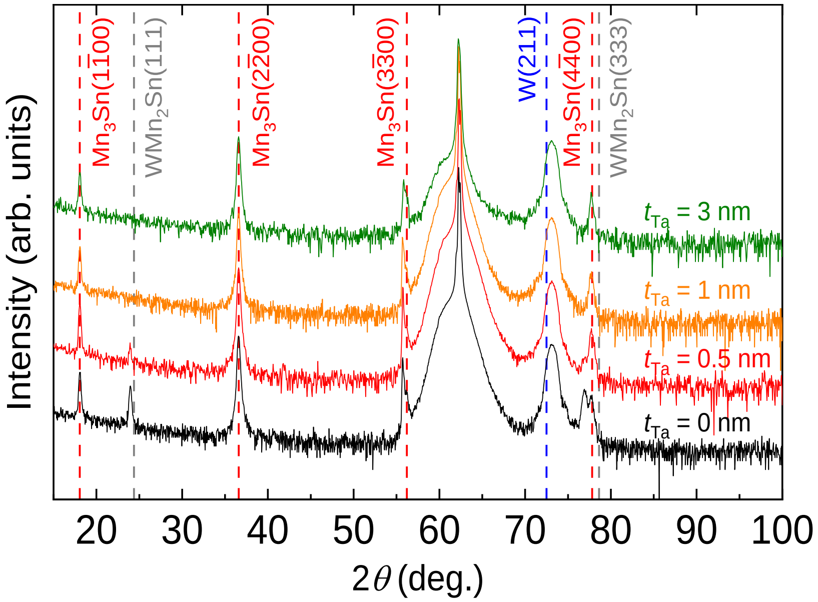

- XRD (Φ scan)

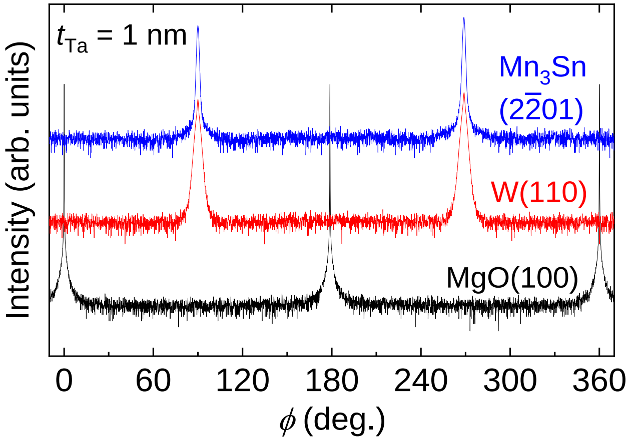

Epitaxial relationship

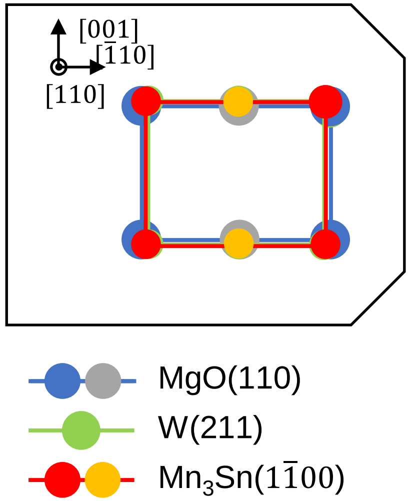

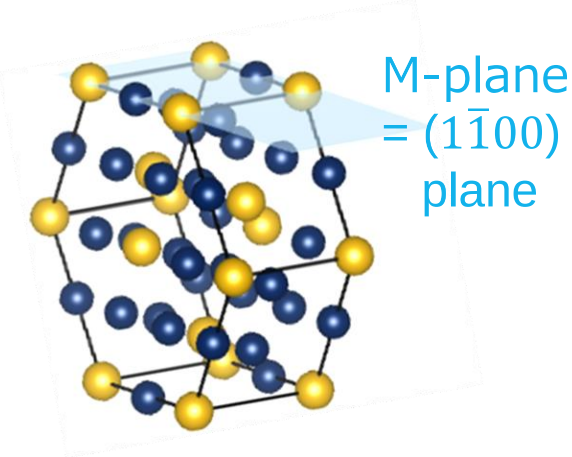

- **W underlayer is suitable to form M-plane-oriented Mn_3Sn.**
- **Insertion of Ta prevents the formation of WMn_2Sn.**
- **Epitaxial relationship:**
  - **MgO(110)[001] ll W(211)$[01\bar{1}]$ ll $Mn_3Sn(1\bar{1}00)[0001]$**

J.-Y. Yoon *et al.*, Appl. Phys. Express **13**, 013001 (2020).

TEM observation of M-plane sample

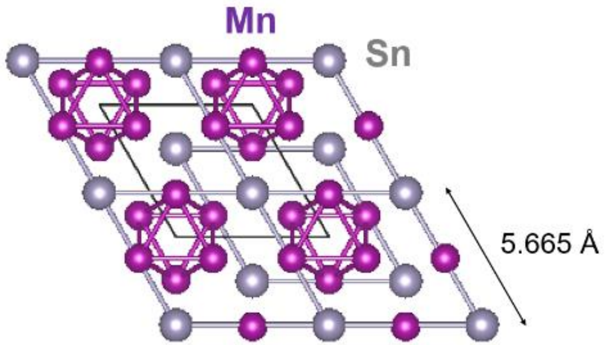

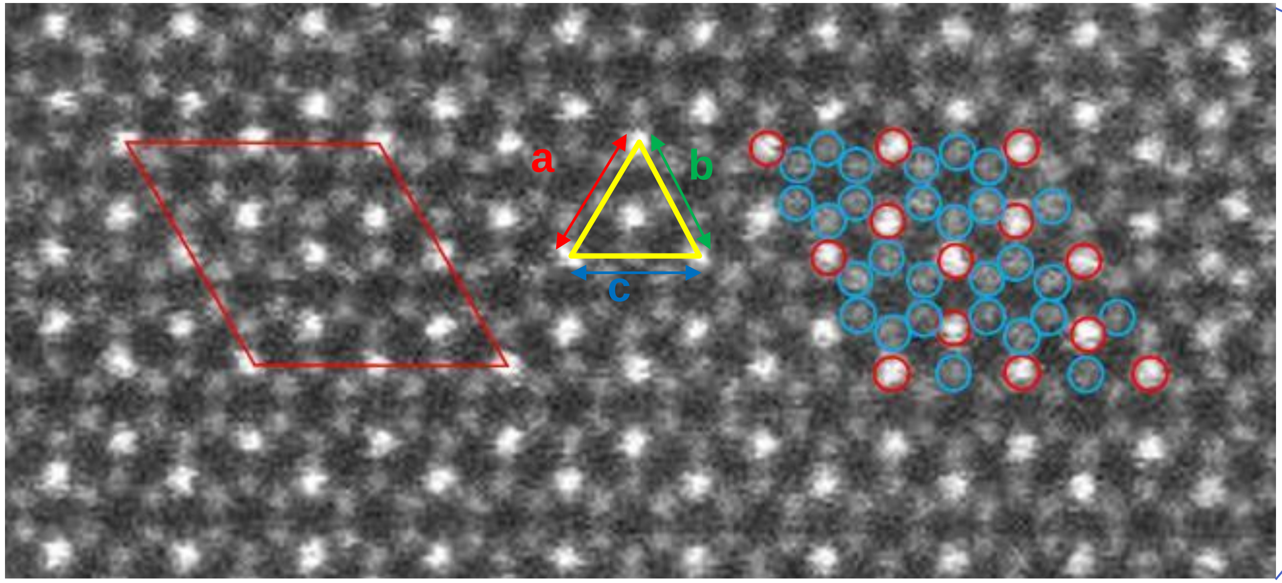

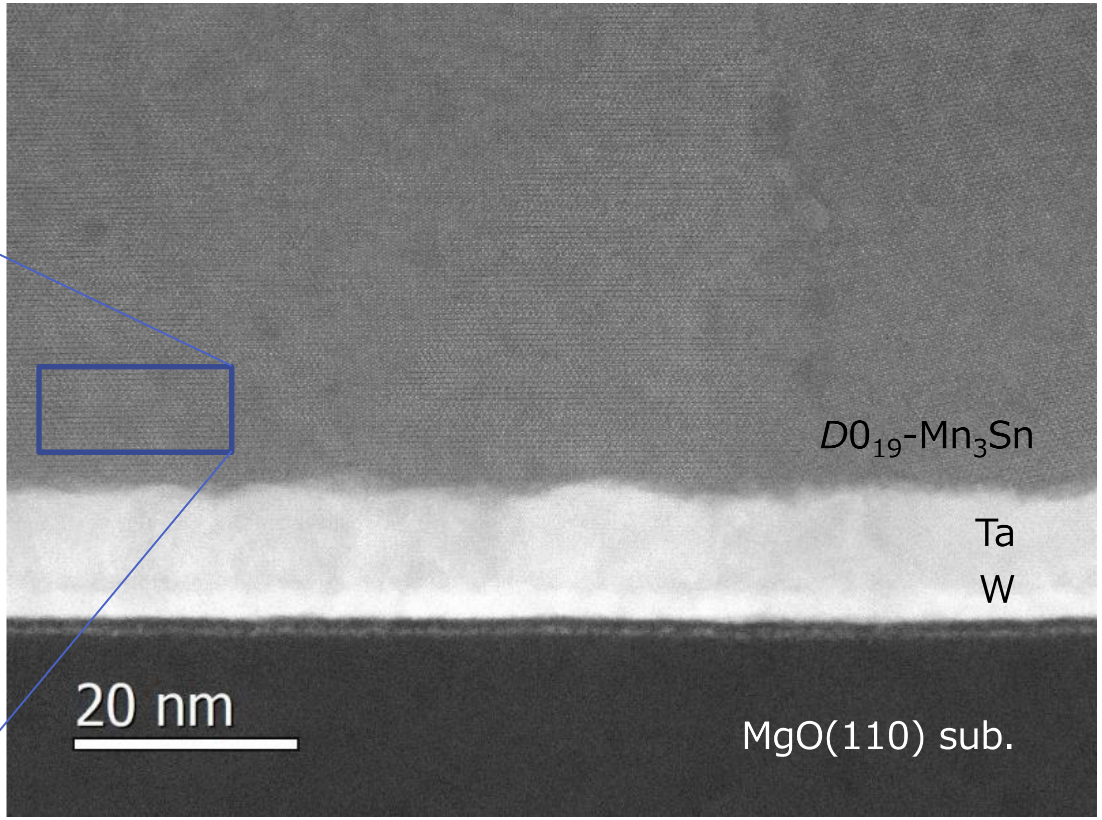

a ≈ 5.6 Å
b ≈ 5.6 Å
c ≈ 5.6 Å

○ : Mn
○ : Sn

Magnetic and magneto-transport properties

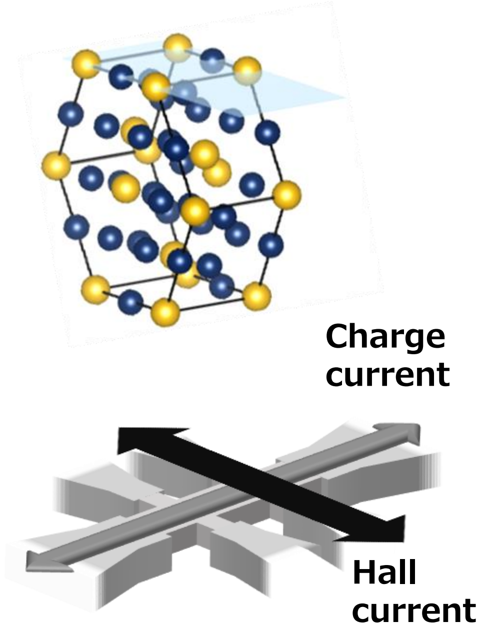

- $M - H$

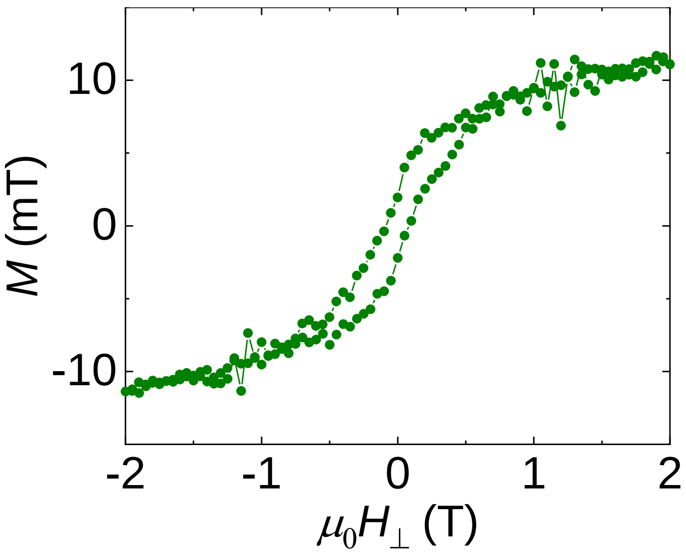

- $\sigma_{xy} - H_\perp$

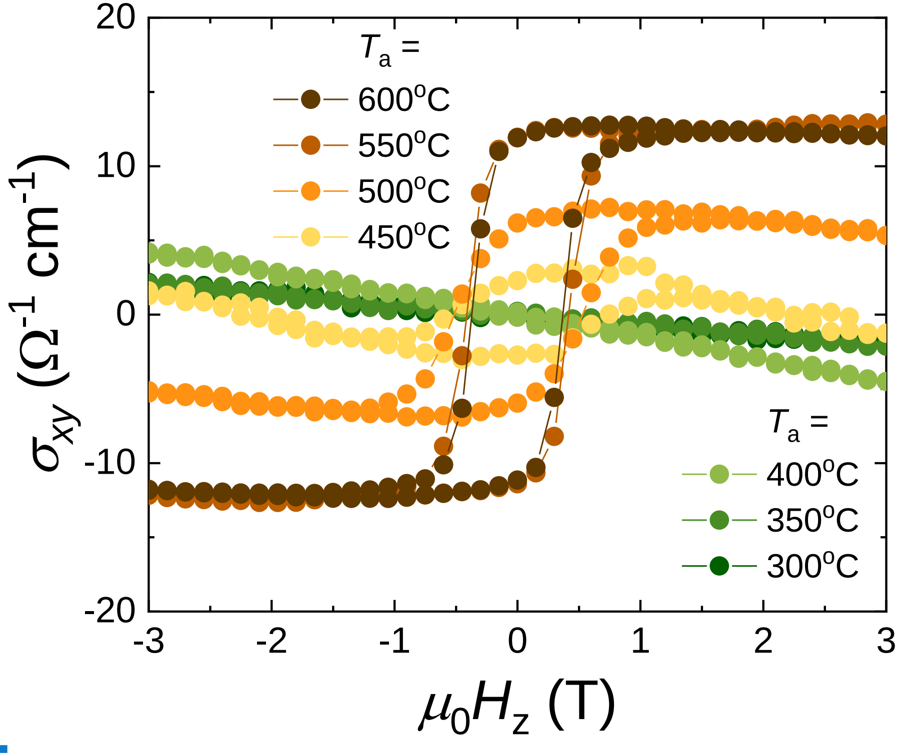

- **Small residual magnetization ~ 5 mT**
- **Large anomalous Hall conductivity ~ 13 $\Omega^{-1}cm^{-1}$ @ high-temperature annealing**

J.-Y. Yoon et al., Appl. Phys. Express **13**, 013001 (2020)
J.-Y. Yoon et al., AIP Adv. **11**, 065318 (2021).

Outline

1. Introduction
   - Electrical manipulation of magnetic materials
   - Non-collinear antiferromagnet
2. Chiral-spin rotation of non-collinear antiferromagnet Mn_3Sn
   - Preparation of epitaxial thin film
   - Chiral-spin rotation
   - Analysis of domain size
   - Mn_3Sn thickness dependence
3. Summary

Sample structure and R_H-H loop

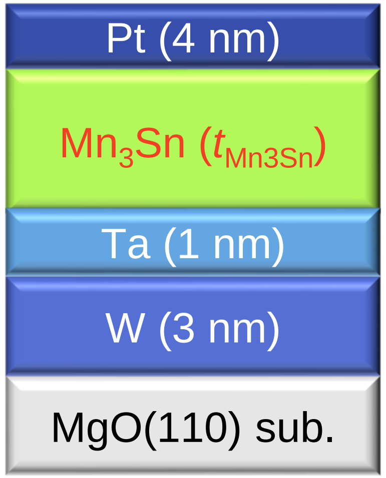

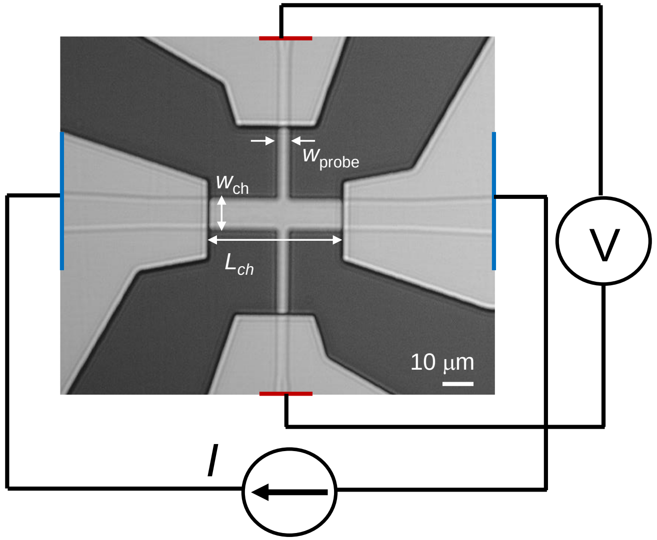

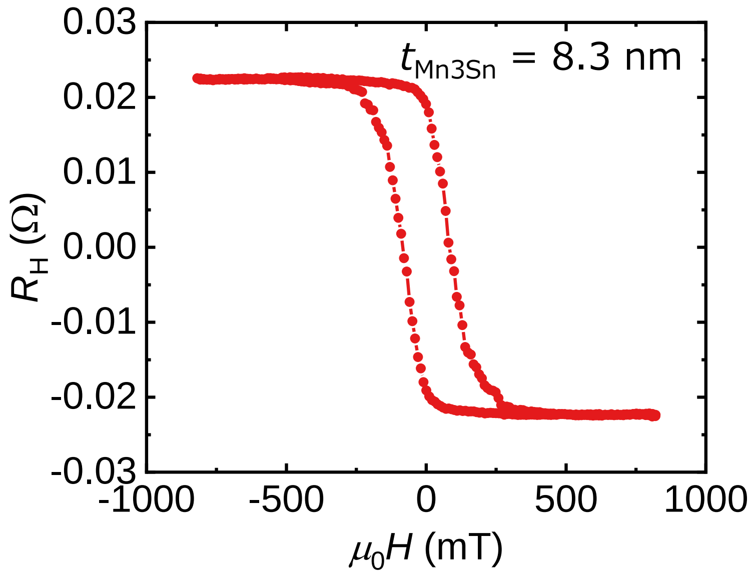

- t_{Mn3Sn}: 8.3 – 22.5 nm
- Sandwiched by Pt and W/Ta
  ➔ Enhanced SOT
- MgO-capped sample is prepared as a reference.

- W_{ch}: 3 – 50 μm
  ➔ Estimation of domain size (presented later)
- L_{ch}: 50 μm
- W_{probe}: 3 μm

- Negative R_H-H loop
  ➔ AHE due to chiral-spin structure
- Square hysteresis even at t_{Mn3Sn} = 8.3 nm

Y. Takeuchi *et al.*, Nat. Mater. (2021) doi.org/10.1038/s41563-021-01005-3

Configurations

s ⊥ kagome plane

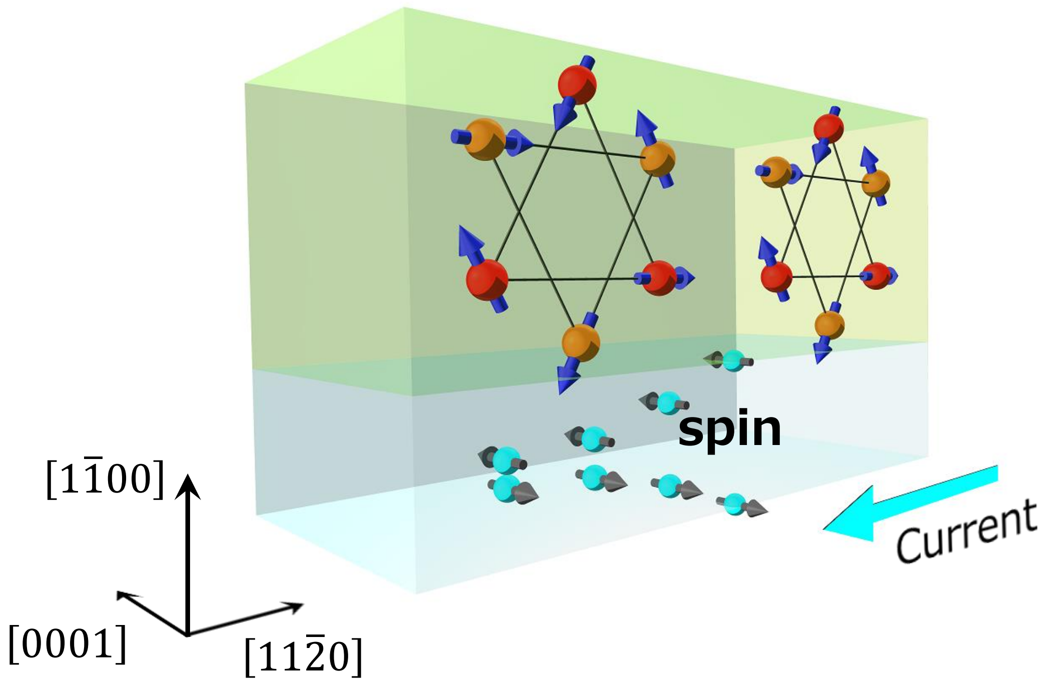

s ∥ kagome plane

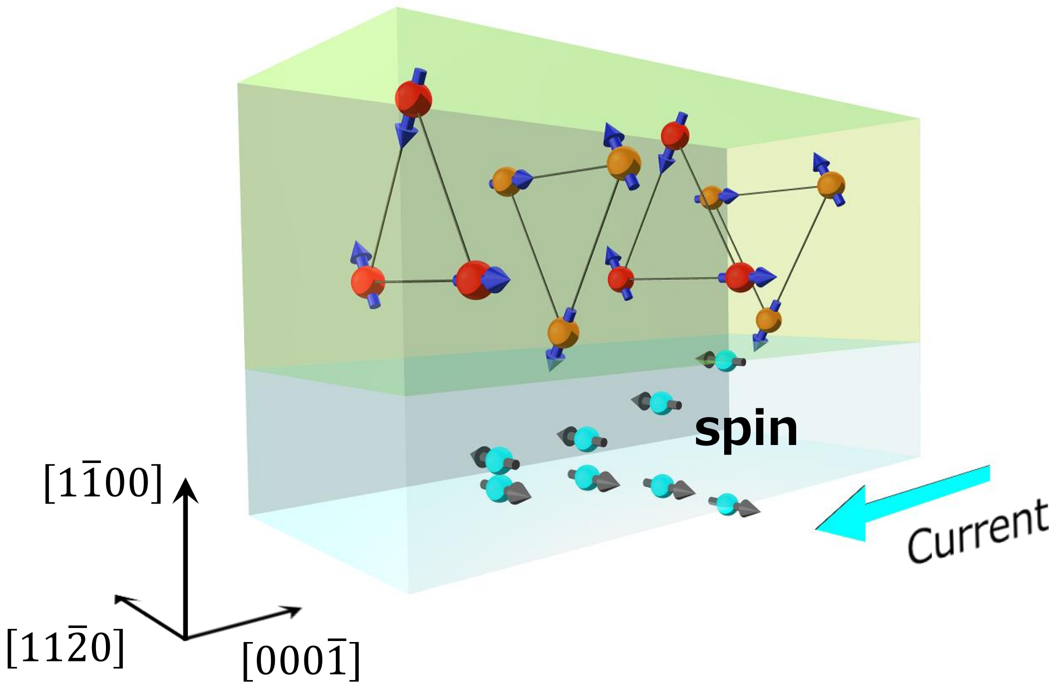

Y. Takeuchi *et al.*, Nat. Mater. (2021) doi.org/10.1038/s41563-021-01005-3

Main result

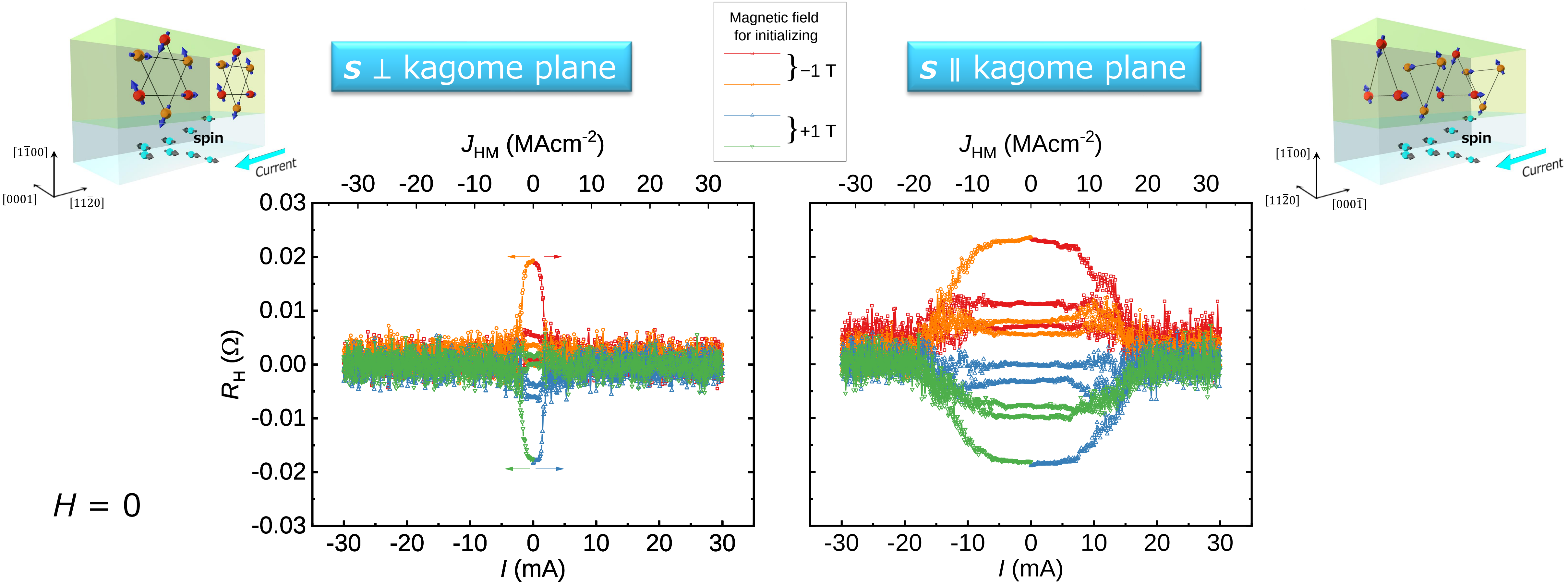

- R_H transits to intermediate level regardless of directions of initialization and current.
- Threshold current is largely different between the two configurations.
- Fluctuation level is largely different below and above the threshold current.

Y. Takeuchi *et al*., Nat. Mater. (2021) doi.org/10.1038/s41563-021-01005-3

Driving force

Cap-layer dependence

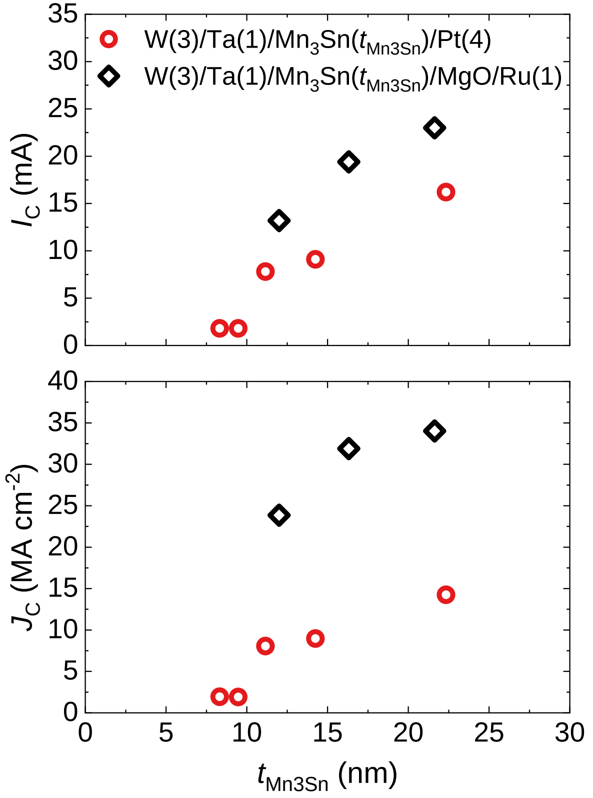

➢ Pt-capped sample shows smaller I_C and J_C.

R_H-H curve under various I

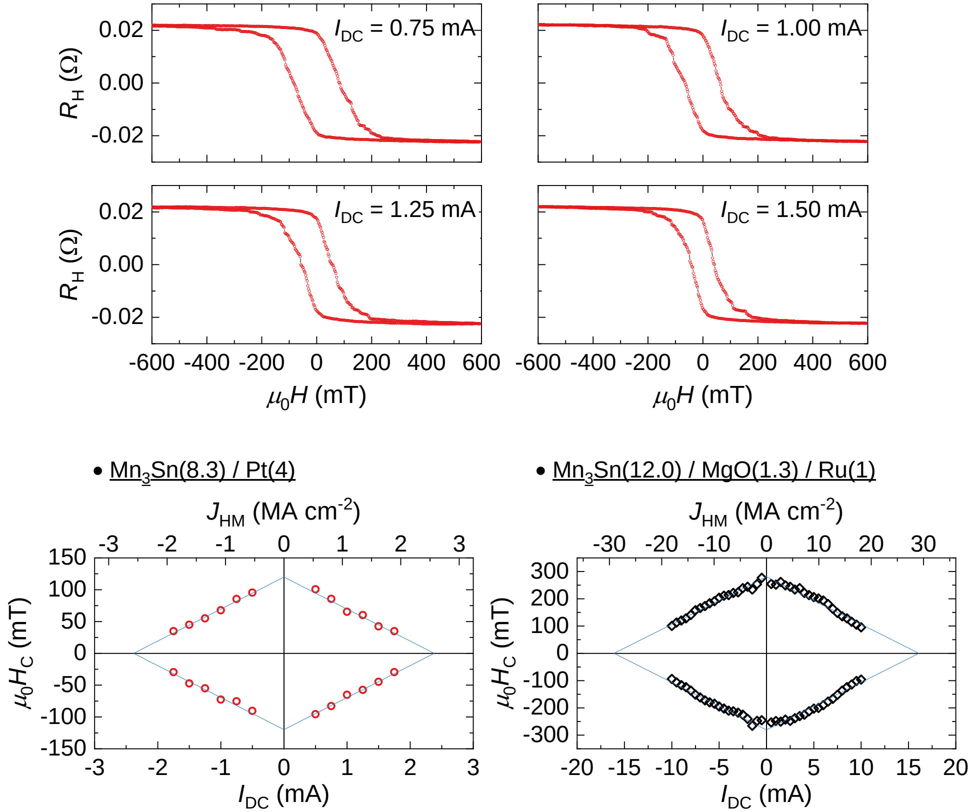

➢ H_C linearly decreases with I.

Joule heating

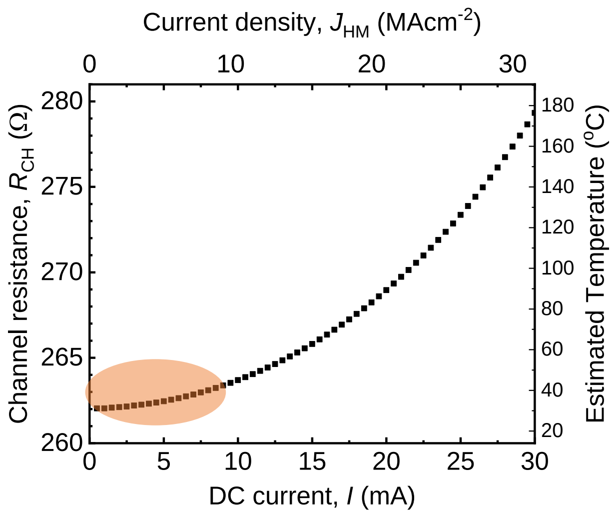

➢ Joule heating plays a negligible role. (ΔT < 11 °C)

SOT plays a dominant contribution.

Y. Takeuchi *et al.*, Nat. Mater. (2021) doi.org/10.1038/s41563-021-01005-3

Possible scenario

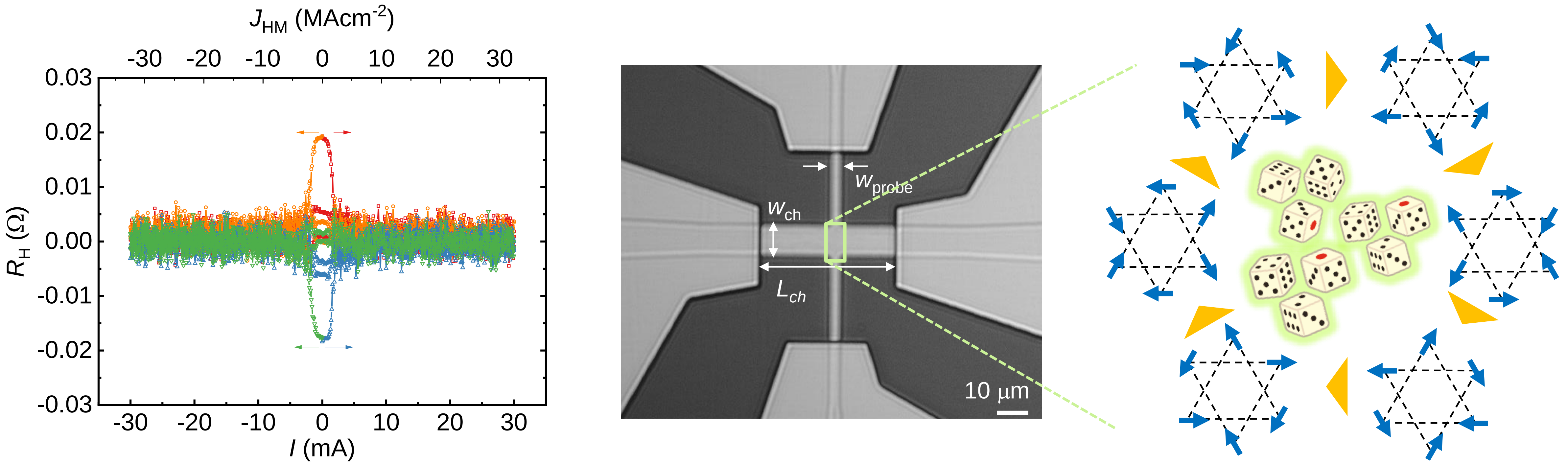

1. **Chiral-spin structure starts with uniform state by initialization.**
2. **Hall cross consists of multiple domains.**
3. **Chiral-spin structure in each domain starts rotating above I_C.**
4. **When I is turned off, each domain settles into one of the six stable points.**
5. **R_H is observed as an average of each domain.**

Y. Takeuchi *et al.*, Nat. Mater. (2021) doi.org/10.1038/s41563-021-01005-3

Chiral-spin LLG simulation

$$\frac{\partial \boldsymbol{m}_\mu}{\partial t} = -\gamma \boldsymbol{m}_\mu \times \boldsymbol{H}_\mu + \alpha \boldsymbol{m}_\mu \times \frac{\partial \boldsymbol{m}_\mu}{\partial t} - \frac{\gamma \hbar \theta_{\mathrm{SH}} J}{2eM_S d} \boldsymbol{m}_\mu \times (\boldsymbol{m}_\mu \times \boldsymbol{s})$$

$$\mu = A, B, C$$

$$\boldsymbol{H}_\mu = -\frac{1}{M_S} \frac{\partial u}{\partial \boldsymbol{m}_\mu}$$

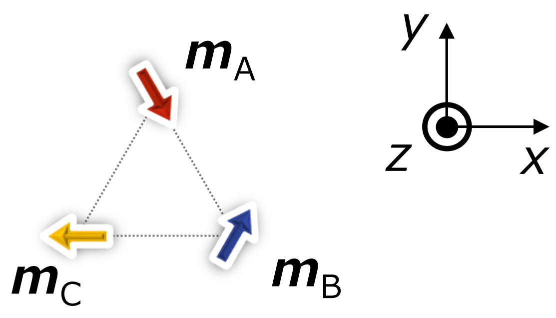

$$u = J_0 \sum_{\langle \mu\nu \rangle} \boldsymbol{m}_\mu \cdot \boldsymbol{m}_\nu + D\boldsymbol{e}_z \sum_{\langle \mu\nu \rangle} \boldsymbol{m}_\mu \times \boldsymbol{m}_\nu - K \sum_{\mu=A,B,C} (\boldsymbol{m}_\mu \cdot \boldsymbol{e}_{K,\mu})^2$$

$$\begin{pmatrix} \boldsymbol{e}_{K,A} = (-\boldsymbol{e}_x + \sqrt{3}\boldsymbol{e}_y)/2 \\ \boldsymbol{e}_{K,B} = -(\boldsymbol{e}_x + \sqrt{3}\boldsymbol{e}_y)/2 \\ \boldsymbol{e}_{K,C} = \boldsymbol{e}_x \end{pmatrix}$$

Y. Yamane, O. Gomonay, J. Sinova, Phys. Rev. B **100**, 054415 (2019).

For this work

- J_0 = 10^8 J m^{-3}
- D = 10^7 J m^{-3}
- K = 1.6×10^6 J m^{-3}
- M_S = 1.26 T

} M = 6 mT

- α = 0.01
- θ_{SH} = 0.15
- d = 10 nm

Calculation results

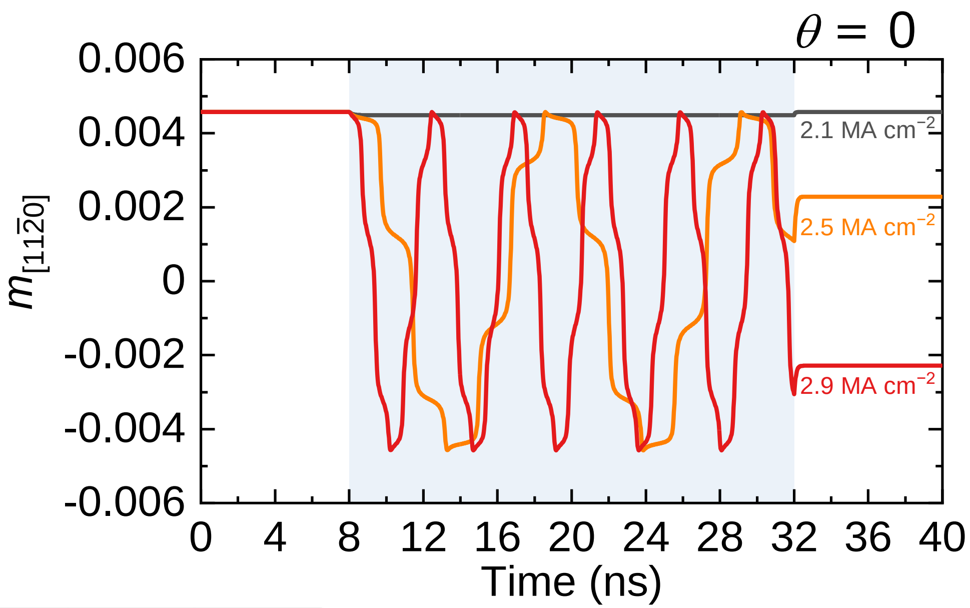

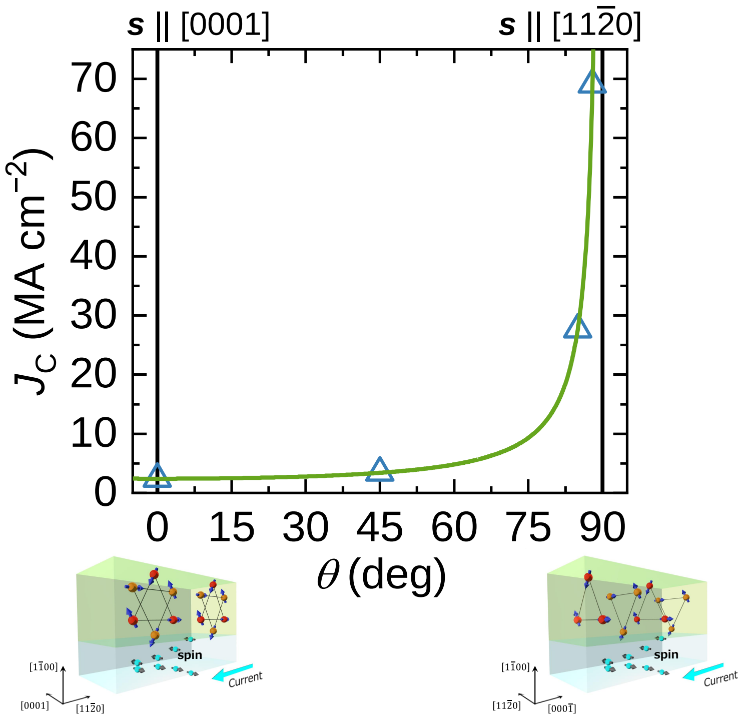

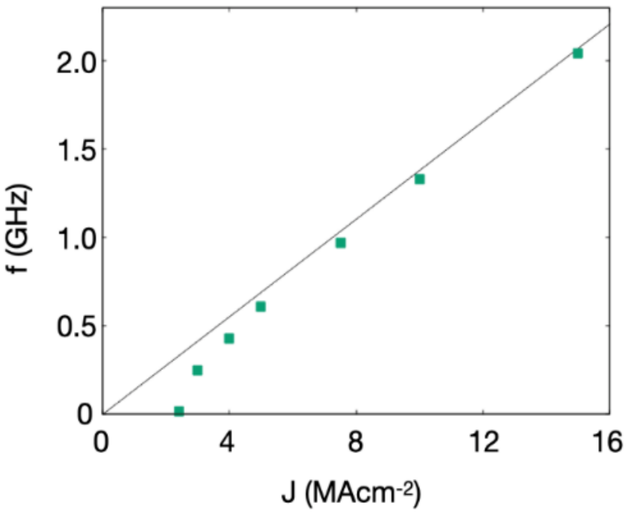

- **Chiral-spin structure oscillates above a threshold.**
- **Frequency varies with the applied current.**
  - **Tunable oscillator?**
- **Threshold current increases with θ, consistent with experiment.**

Y. Takeuchi *et al.*, Nat. Mater. (2021) doi.org/10.1038/s41563-021-01005-3

Rotation vs. Reversal (Tsai *et al.* 2020)

s ⊥ kagome plane

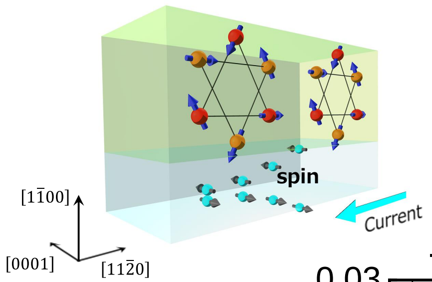

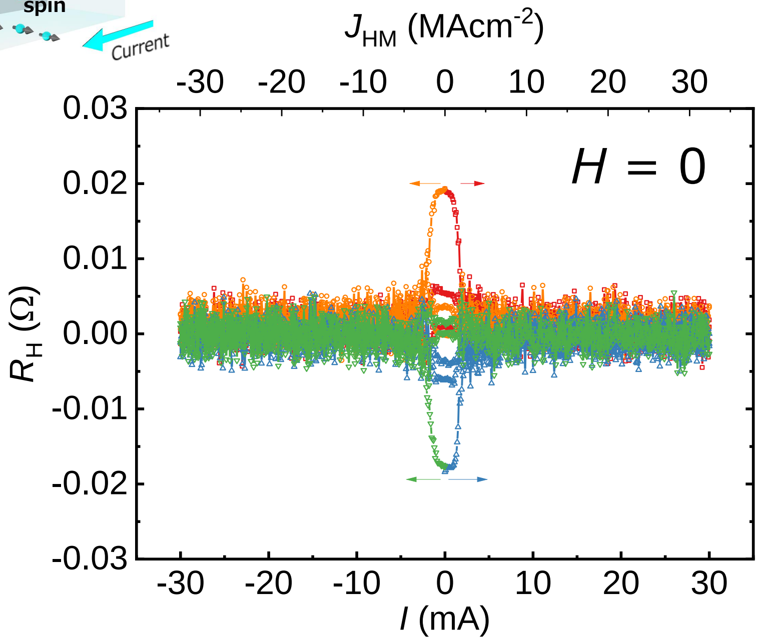

s ∥ kagome plane

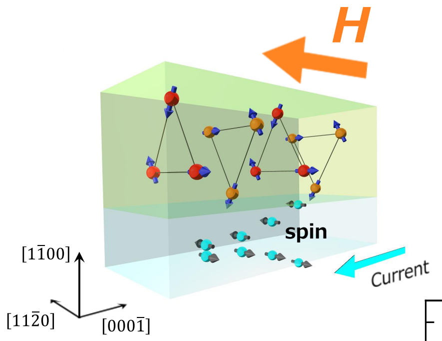

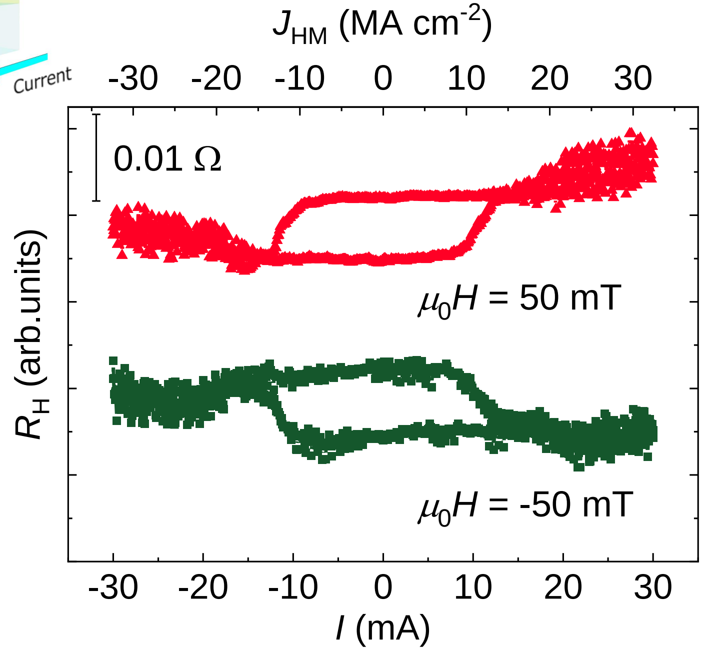

Continuous rotation	Bipolar switching
$H = 0$	$H_X \neq 0$
$J_C \sim 1$ MA/cm^2	$J_C \sim 10$ MA/cm^2

Y. Takeuchi *et al.*, Nat. Mater. (2021) doi.org/10.1038/s41563-021-01005-3

Outline

1. **Introduction**
   - Electrical manipulation of magnetic materials
   - Non-collinear antiferromagnet
2. **Chiral-spin rotation of non-collinear antiferromagnet Mn_3Sn**
   - Preparation of epitaxial thin film
   - Chiral-spin rotation
   - Analysis of domain size
   - Mn_3Sn thickness dependence
3. **Summary**

Quantification of domain size – concept

Narrower wire

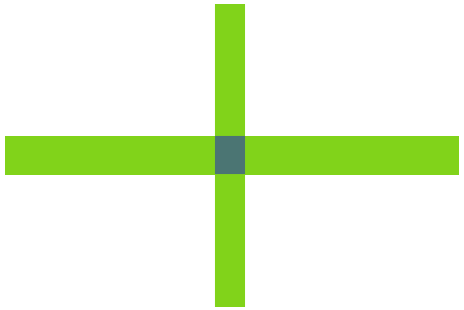

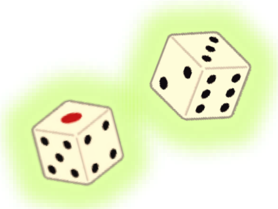

Wider wire

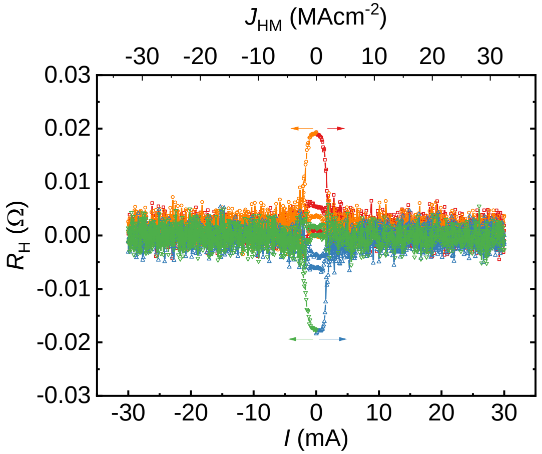

Fewer domains
➔Larger R_H fluctuation

More domains
➔Smaller R_H fluctuation

Fluctuation level → Mean domain size

Y. Takeuchi *et al*., Nat. Mater. (2021) doi.org/10.1038/s41563-021-01005-3

Quantification of domain size – result

$$\sigma_{\mathrm{SOT}}^2 = \sigma_{\mathrm{High}\,I}^2 - \sigma_{\mathrm{Low}\,I}^2$$

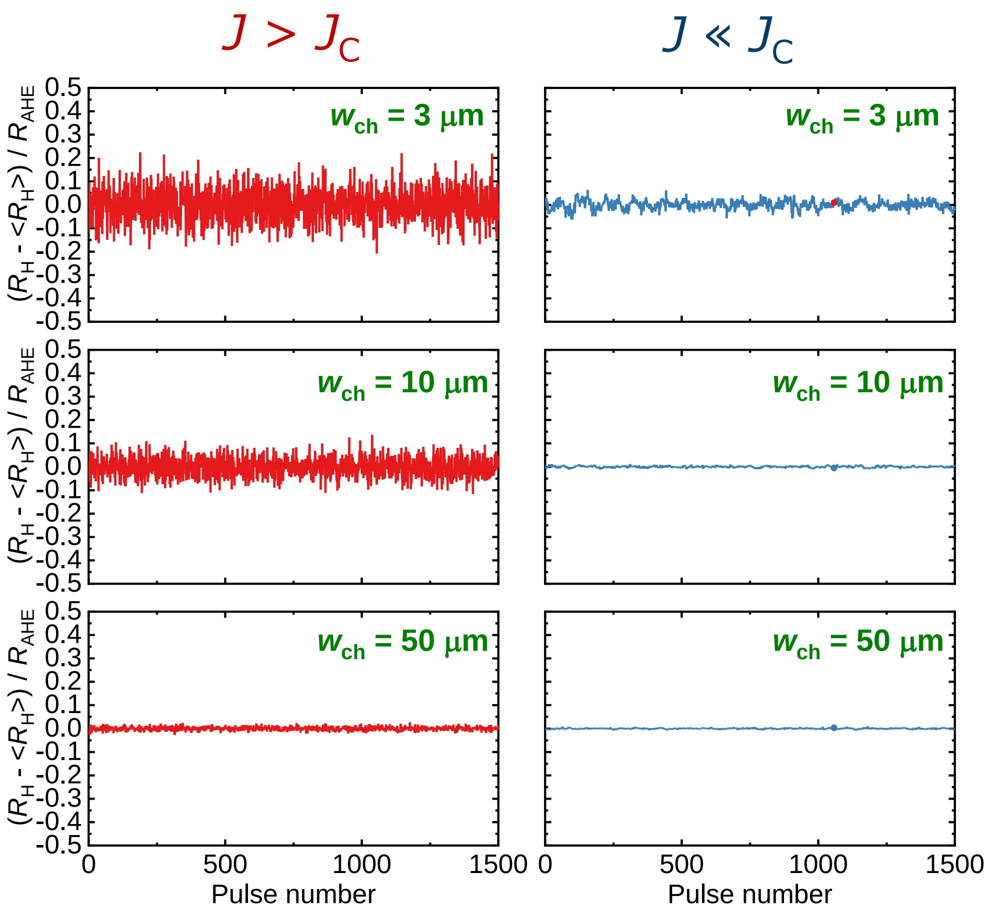

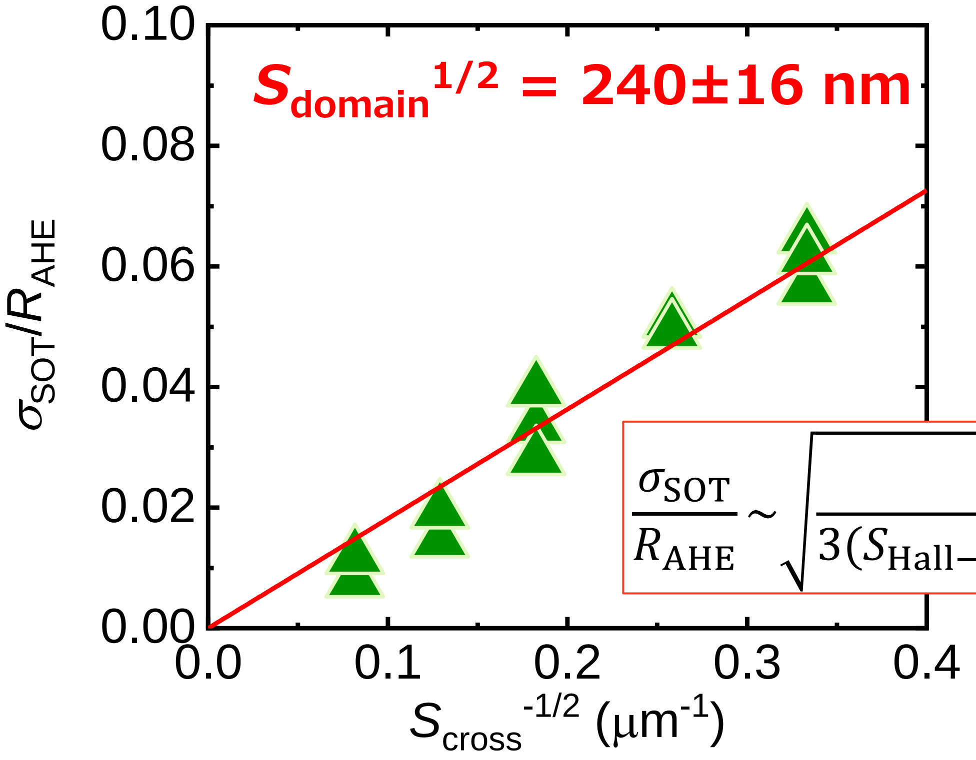

$$\frac{\sigma_{\mathrm{SOT}}}{R_{\mathrm{AHE}}} \sim \sqrt{\frac{2}{3(S_{\mathrm{Hall-Cross}}/S_{\mathrm{domain}})}}$$

- Good agreement with a scale suggested from W-dependent H_{C}.

H. Bai *et al.*, Appl. Phys. Lett. **117**, 052404 (2020).

Y. Takeuchi *et al.*, Nat. Mater. (2021) doi.org/10.1038/s41563-021-01005-3

Outline

1. Introduction
   - Electrical manipulation of magnetic materials
   - Non-collinear antiferromagnet
2. Chiral-spin rotation of non-collinear antiferromagnet Mn_3Sn
   - Preparation of epitaxial thin film
   - Chiral-spin rotation
   - Analysis of domain size
   - Mn_3Sn thickness dependence
3. Summary

Spin torque on AFM

nature materials ARTICLES
https://doi.org/10.1038/s41563-018-0236-9

Long spin coherence length and bulk-like spin–orbit torque in ferrimagnetic multilayers

Jiawei Yu[1], Do Bang[2,3,8], Rahul Mishra[1,8], Rajagopalan Ramaswamy[1], Jung Hyun Oh[4], Hyeon-Jong Park[5], Yunboo Jeong[6], Pham Van Thach[2,3], Dong-Kyu Lee[4], Gyungchoon Go[4], Seo-Won Lee[4], Yi Wang[1], Shuyuan Shi[1], Xuepeng Qiu[7], Hiroyuki Awano[2], Kyung-Jin Lee[4,5,6]* and Hyunsoo Yang[1]*

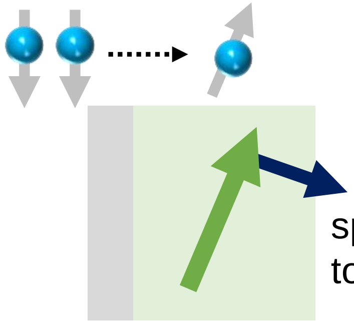

$$\lambda_C = \frac{\pi}{\left|k_F^{\uparrow} - k_F^{\downarrow}\right|}$$

- FM: $k_F^{\uparrow} \neq k_F^{\downarrow}$ ➔ Surface torque
- AFM: $k_F^{\uparrow} = k_F^{\downarrow}$ ➔ Bulk-like torque

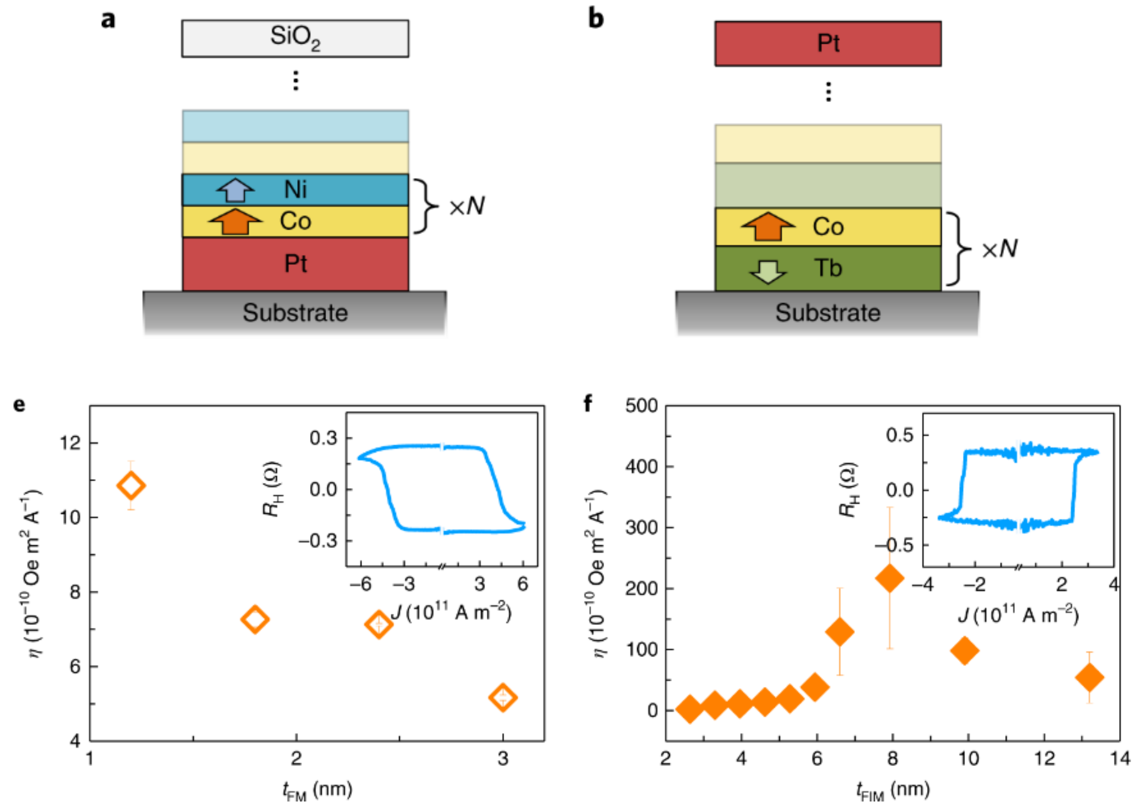

- **Switching efficiency**
  - **Ferri: Large and increases with *t* up to 8 nm**
  - **Ferro: Small and decreases with *t***

➡ **How about in NC-AFM?**

J. Yu *et al.*, NMAT **18**, 29 (2019).

Switching efficiency vs. t_{Mn3Sn}

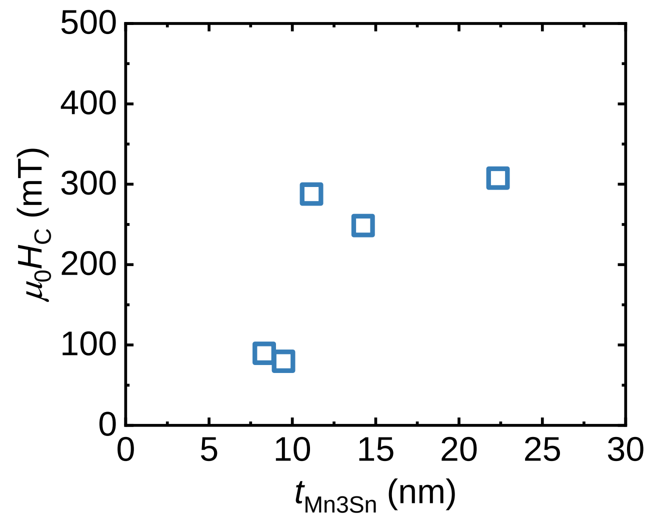

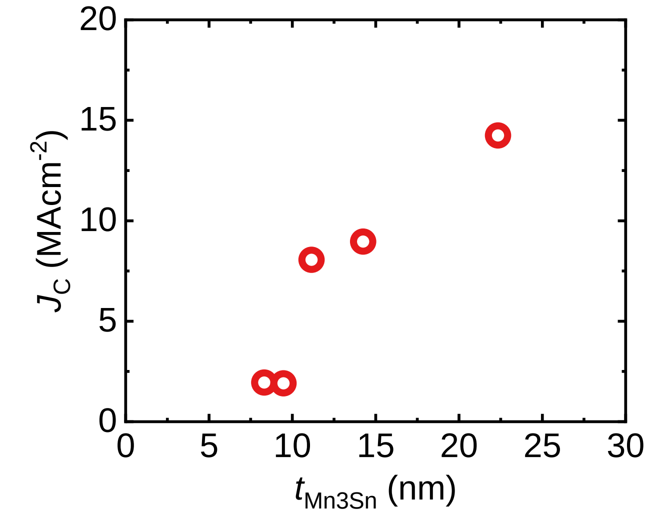

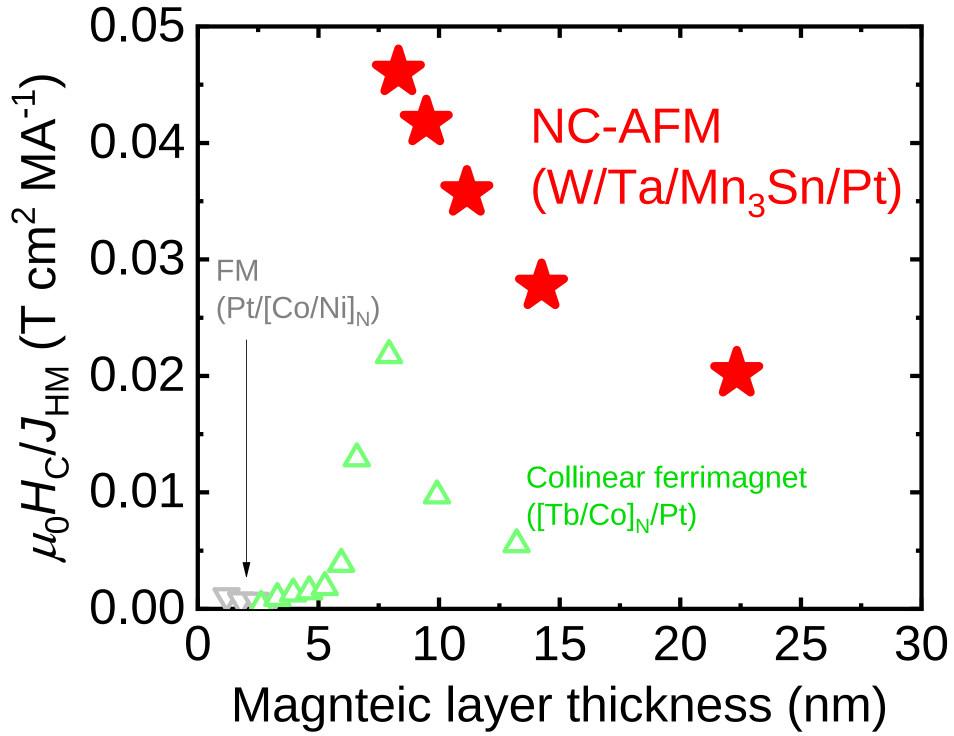

- **Follows 1/*t* relation.**
- **Larger than FM and collinear ferrimagnet.**

Y. Takeuchi *et al.*, Nat. Mater. (2021) doi.org/10.1038/s41563-021-01005-3

Why efficient in NC-AFM?

i. Field-driven dynamics

- Out-of-kagome-plane anisotropy
- Small net magnetization

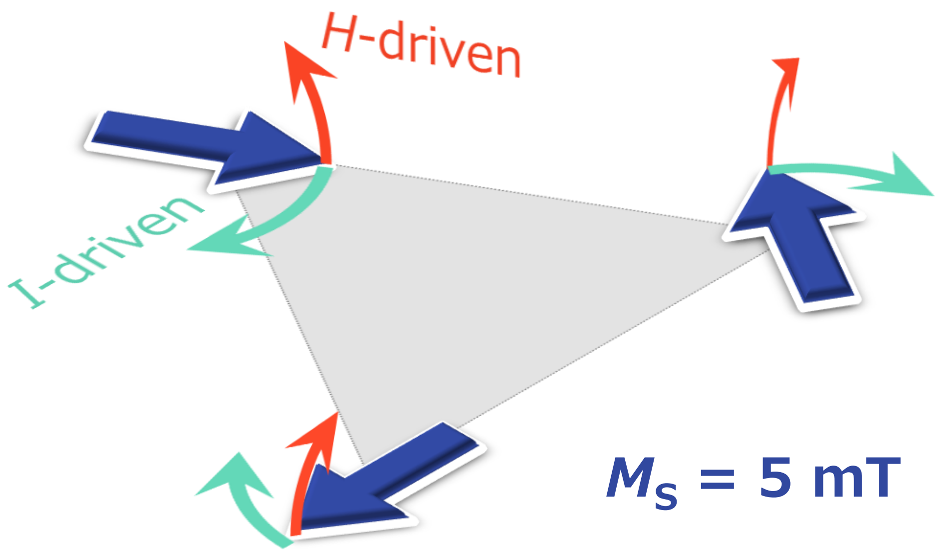

ii. Current-driven dynamics

- In-kagome-plane anisotropy

Y. Takeuchi *et al*., Nat. Mater. (2021) doi.org/10.1038/s41563-021-01005-3

Outline

1. Introduction
   - Electrical manipulation of magnetic materials
   - Non-collinear antiferromagnet
2. Chiral-spin rotation of non-collinear antiferromagnet Mn_3Sn
   - Preparation of epitaxial thin film
   - Chiral-spin rotation
   - Analysis of domain size
   - Mn_3Sn thickness dependence
3. Summary

Summary

■ Epitaxial M-plane-oriented Mn_3Sn thin film

- ➢ Prepared on MgO(110) substrate with W/Ta buffer layer.

J.-Y. Yoon *et al.*, Appl. Phys. Express **13**, 013001 (2020).
J.-Y. Yoon *et al.*, AIP Advances **11**, 065318 (2021).

■ Chiral-spin rotation

- ➢ Transition and fluctuation of Hall resistance are observed above a threshold.
- ➢ Threshold current depends on the Kagome-plane orientation.
- ➢ Consistently explained by a **chiral-spin rotation** induced by SOT.
  - Chiral-spin rotation requires no field and smaller current, compared with reversal.
- ➢ Domain size estimated as 240 nm from the fluctuation level vs. wire width.
- ➢ Higher switching efficiency than collinear systems.

Y. Takeuchi, Y. Yamane, J.-Y. Yoon, R. Itoh, B. Jinnai, S. Kanai, J. Ieda, S. Fukami, and H. Ohno,
"Chiral-spin rotation of non-collinear antiferromagnet by spin-orbit torque"
Nature Materials (2021) doi.org/10.1038/s41563-021-01005-3.

End